AD-A128 510 HOLOGRAPHIC METHODS FOR THE INVESTIGATION OF PHOTOPHYSICAL PROPERTIES(U) IBM RESEARCH LAB SAN JOSE CA C BRAEUCHLE ET AL. 22 APR 83 TR-4 N00014-81-C-0418 1/1

UNCLASSIFIED F/G 7/5 NL

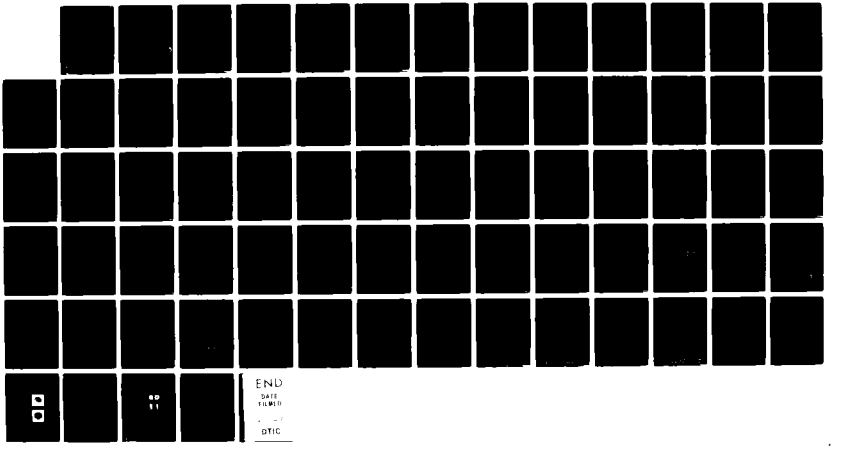

END
DATE FILMED
DTIC

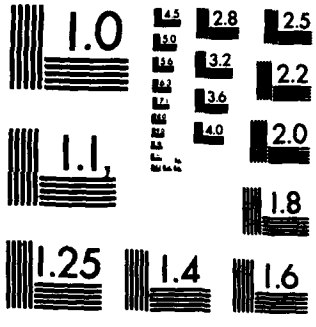

Unclassified

SECURITY CLASSIFICATION OF THIS PAGE (When Data Entered)

REPORT DOCUMENTATION PAGE		READ INSTRUCTIONS BEFORE COMPLETING FORM
1. REPORT NUMBER: 4	2. GOVT ACCESSION NO.: AD A128510	3. RECIPIENT'S CATALOG NUMBER
4. TITLE (and Subtitle): HOLOGRAPHIC METHODS FOR THE INVESTIGATION OF PHOTOPHYSICAL PROPERTIES		5. TYPE OF REPORT & PERIOD COVERED: Technical Report
		6. PERFORMING ORG. REPORT NUMBER
7. AUTHOR(s): Chr. Bräuchle and D. M. Burland		8. CONTRACT OR GRANT NUMBER(s): N00014-81-C-0418
9. PERFORMING ORGANIZATION NAME AND ADDRESS: International Business Machines Corp. San Jose Research Laboratory 5600 Cottle Road, San Jose, CA 95193		10. PROGRAM ELEMENT, PROJECT, TASK AREA & WORK UNIT NUMBERS: 051-782
11. CONTROLLING OFFICE NAME AND ADDRESS: Office of Naval Research Code 413 800 N. Quincy Street Arlington, VA 22217		12. REPORT DATE: April 22, 1983
		13. NUMBER OF PAGES: 68
14. MONITORING AGENCY NAME & ADDRESS(if different from Controlling Office)		15. SECURITY CLASS. (of this report): Unclassified
		15a. DECLASSIFICATION/DOWNGRADING SCHEDULE

16. DISTRIBUTION STATEMENT (of this Report)

This document has been approved for public release and sale; its distribution is unlimited.

17. DISTRIBUTION STATEMENT (of the abstract entered in Block 20, if different from Report)

18. SUPPLEMENTARY NOTES

To be published in Angewandte der Chemie

19. KEY WORDS (Continue on reverse side if necessary and identify by block number)

Holography, photochemistry, kinetics

20. ABSTRACT (Continue on reverse side if necessary and identify by block number)

Holography is most frequently thought of as a method of photography that results in three-dimensional images of the object being photographed. It is certainly true that this is the most visually spectacular aspect. But holography can also be used as a powerful tool for the investigation of a variety of photochemical and photophysical processes. These experimental techniques rely on the fact that small spatial modulations of a material's optical

DD FORM 1 JAN 73 1473 EDITION OF 1 NOV 65 IS OBSOLETE S/N 0102-LF-014-6601

Unclassified

SECURITY CLASSIFICATION OF THIS PAGE (When Data Entered)

20. properties (index of refraction and absorption coefficient) can deflect an incident light beam into another direction. By following the growth or decay in intensity of this deflected beam, one can follow the underlying physical process producing the changes in optical properties. If a cw laser is used to produce the hologram one can use the technique to investigate solid state photochemistry. If a pulsed laser is used one can investigate a broad range of time dependent processes; energy transfer, diffusion, rotational relaxation, charge transport, etc.

As a result of information obtained using the holographic technique as a scientific tool, one can also find new classes of materials for the recording of holograms. This is the way in which two-photon four-level systems for hologram recording in the infrared were discovered. Materials of this type are self-developing, can have the recording process gated on and off with an auxiliary source and can be read with the infrared recording laser with no erasing of the hologram.

OFFICE OF NAVEL RESEARCH

Contract N00014-81-C-0418

Task No. NR 051-782

TECHNICAL REPORT NO. 4

Holographic Methods for the Investigation of Photophysical Properties

by

Chr. Brauchle and D. M. Burland

Prepared for Publication

in

Angewandte der Chemie

IBM Research Laboratory
San Jose, California 95193

April 22, 1983

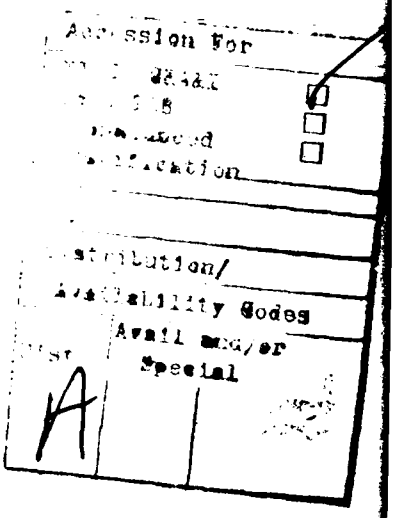

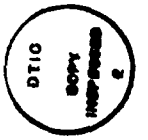

RJ 3869 (44066) 4/22/83
Chemistry

HOLOGRAPHIC METHODS FOR THE INVESTIGATION OF PHOTOPHYSICAL PROPERTIES

Chr. Bräuchle

Institut für Physikalische Chemie
Universität München,
D-8000 Munich 2, FRG

D. M. Burland

IBM Research Laboratory
San Jose, California 95193

ABSTRACT: Holography is most frequently thought of as a method of photography that results in three-dimensional images of the object being photographed. It is certainly true that this is the most visually spectacular aspect. But holography can also be used as a powerful tool for the investigation of a variety of photochemical and photophysical processes. These experimental techniques rely on the fact that small spatial modulations of a material's optical properties (index of refraction and absorption coefficient) can deflect an incident light beam into another direction. By following the growth or decay in intensity of this deflected beam, one can follow the underlying physical process producing the changes in optical properties. If a cw laser is used to produce the hologram one can use the technique to investigate solid state photochemistry. If a pulsed laser is used one can investigate a broad range of time dependent processes; energy transfer, diffusion, rotational relaxation, charge transport, *etc.*

As a result of information obtained using the holographic technique as a scientific tool, one can also find new classes of materials for the recording of holograms. This is the way in which two-photon four-level systems for hologram recording in the infrared were discovered. Materials of this type are self-developing, can have the recording process gated on and off with an auxiliary source and can be read with the infrared recording laser with no erasing of the hologram.

1. INRODUCTION

Holography is most widely known as a technique for producing a three-dimensional picture. According to Gaboı's original idea,[1] for which he received the Nobel prize in 1971, a picture or more generally information can be stored as an interference pattern generated from an object and reference wave. Although the production of a three-dimensional picture[2] was one of the most impressive initial results of holography,[3-5] applications of the technique have spread over a variety of different areas since. For example, holographic interferometry[6,7] can be used to measure very small deformations of an object which is put under mechanical stress. In this way holography represents an important advance in nondestructive material testing. Medical and biomedical applications[8] are a growing field for holographic methods. A great amount of effort has also gone into the assessment of the potential usefulness of holograms in optical memories.[9,10] In this application holograms containing *binary information* are produced in a two- or three-dimensional array. Holograms can play an important role in coherent optical data processing.[11,12] Perhaps in the future holograms will be most widely used for the production of a variety of kinds of optical elements for focusing and deflecting light.[13,14] Holographic optical elements are currently being considered for applications as passive devices in the fast growing area of integrated optics[15] and optical communication technologies.[16]

In all of these cases the basic principle[3-5] is the same: An object wave which carries complete information about the object in the modulation of its intensity and phase is overlapped with a reference wave (see Fig. 1a) which is frequently a plane wave. If both waves are mutually *coherent* in space and time, *i.e.*, if there are fixed phase relationships between both waves during the recording period, a stationary pattern is produced. This pattern can be impressed photochemically into a photosensitive recording medium. The

photochemically stored interference pattern is called the hologram. It consists of a complex pattern of irregularly arranged bright and dark regions of microscopic dimensions representing the interference fringes. Because of this irregularity such a hologram at first sight seems to contain no information at all. However, if it is illuminated with the reference wave only (see Fig. 1b), the recorded interference fringes diffract part of the reference wave in such a way that an image wave is reconstructed as an exact replica of the original object wave. Since not only the intensity (as in photography) but also the absolute value of the phase of the object wave is reconstructed correctly, the technique is called holography, originating from the Greek word "holos" meaning "the whole". A hologram permits one to reconstruct a complete three-dimensional picture of the original object.

From this brief description of holography it is obvious that *coherence* of the object and reference wave is a prerequisite. Therefore after the invention of holography[1] in 1948 its rapid development had to await the development of the laser[17] as a source of coherent light. The close relationship between laser technology and holographic development holds to the present day. So, for example, new lasers such as the semiconductor lasers[18] have stimulated a search for new holographic recording materials in the infrared.

In this review we will concentrate on two aspects of holography. First we want to discuss the application of holography as a scientific tool for the investigation of photochemical and photophysical processes. Because the hologram recording process involves photochemical and photophysical changes in the photosensitive molecules of the recording medium, it is possible to use holography in order to follow these processes. In this way, holography can serve as an extremely sensitive tool for fundamental photochemical and photophysical investigations. The second aspect of holography that we wish to discuss is the search for new holographic recording materials. We will show how fundamental

investigations using holographic photochemistry can yield new kinds of holographic recording materials. These new materials rely on a two-photon four-level (2P4L) photochemical reaction scheme and a comparison with conventional one-photon two-level (1P2L) photochemical recording systems will demonstrate that the 2P4L systems have many significant advantages. The use of these new materials in a range of holographic applications will be discussed.

II. THE USE OF HOLOGRAPHY TO INVESTIGATE PHOTOCHEMICAL AND PHOTOPHYSICAL PROCESSES

1. The Principle

In order to investigate photochemical and photophysical processes by holography it is reasonable to use the simplest of holograms, *i.e.*, a plane wave hologram.[3-5] This will avoid unnecessary complications. The production of such a plane wave hologram is shown in Fig. 2. Two coherent waves (reference and object wave) with the intensities I_R and I_0 and the same wavelength overlap at the holographic sample. Since both waves are plane waves the interference pattern is a simple cosine modulation of intensity I(x) in the x-direction across the sample

$$I(x) = (I_R + I_0)\left[1 + V\cos\left(\frac{2\pi x}{\Lambda}\right)\right] \qquad (1)$$

where $V = \sqrt{I_R I_0}/(I_R + I_0)$ accounts for the contrast or fringe visibility and $\Lambda = \lambda/(2\sin\theta)$ gives the fringe spacing which is dependent on the wavelength λ and the angle of incidence θ. With both beams having the same intensity ($I_R = I_0$), V equals unity and totally dark and maximally bright stripes occur in the interference pattern, as schematically indicated in Fig. 2.

If the holographic sample contains molecules that are photochemically or photophysically sensitive to the incident light they will change their chemical or physical properties. This change will be strongest in the brightest regions of the interference pattern and absent in the dark regions. In cases where these photochemical or photophysical changes are related to corresponding changes of the index of refraction n or the absorbance a of the molecules, a spatial modulation of the index of refraction

$$n(x) = n_0 + n_1 \cos\left(\frac{2\pi x}{\Lambda}\right) \tag{2a}$$

and the absorbance

$$a(x) = a_0 + a_1 \cos\left(\frac{2\pi x}{\Lambda}\right) \tag{2b}$$

will be produced by the interfering light beams. This modulation has the same periodic behavior as the intensity pattern I(x) in Eq. (1). n_0 and a_0 in Eqs. (2) are the average values of the index of refraction and the absorbance whereas n_1 and a_1 are the corresponding amplitudes of modulation. This photochemically or photophysically impressed variation of the index of refraction or the absorbance into the holographic sample represents the process of recording a plane wave hologram. Because of its regular spatial variation and its analogies to optical gratings it has also been called a holographic grating. When a reading beam strikes such a plane wave hologram along the direction of the reference wave, some of the light from this beam will be diffracted by the holographic grating and the absent object wave will be reconstructed.

A hologram can be characterized by its diffraction efficiency[3] which is defined as the intensity I of the diffracted beam divided by the intensity I_R of the reading beam.

Kogelnik[19] has obtained an important expression for the diffraction of efficiency η of a plane wave hologram of thickness d:

$$\eta = \frac{I}{I_R} = \left[\sin^2\left(\frac{\pi n_1 d}{\lambda' \cos\theta}\right) + \sinh^2\left(\frac{a_1 d}{2\cos\theta}\right)\right] \exp\left(-\frac{2a_0 d}{\cos\theta}\right). \qquad (3a)$$

This expression was derived for thick or volume plane wave holograms for which the relation $d >> \Lambda$ holds. In all cases treated in this review, thick holograms are obtained since, for optical wavelengths and reasonable angles of incidence, Λ is in in the range of several μm which is smaller than d. λ' in Eq. (3a) is the reading wavelength which is not necessarily equal to the writing wavelength λ. Equation (3a) assumes that the reading beam enters at the Bragg angle θ for the particular wavelength λ'.[3,19]

In order to give an interpretation of Eq. (3a) it is important to emphasize that the two terms inside the square bracket of Eq. (3a) represent two different mechanisms of hologram formation. The first term describes hologram formation as a result of changes in the index of refraction and connects the diffraction efficiency with the amplitude n_1 in Eq. (2a). Holograms of this type are called *phase holograms*[3] because the diffraction is caused by phase changes of the reading beam due to the modulation of the optical path lengths by n(x). The second term describes holograms resulting from changes in the absorption coefficient according to Eq. (2b). These holograms are called *amplitude holograms.*[3] For these holograms the diffraction occurs because the reading beam sees a quasi-multislit grating produced by a(x). The exponential factor in Eq. (3a) accounts for the absorption of the reconstruction wave as it passes through the sample. This factor is responsible for the low maximum theoretical diffraction efficiency[3] of 3.7% for a thick amplitude hologram. On the other hand, for pure phase holograms the efficiency may approach 100% if the reading wavelength λ' is not absorbed ($a_0=0$, $a_1=0$). It can be shown[20] that even in cases where

some absorption is present the effect of the phase hologram generally exceeds that of the amplitude hologram. Therefore, when holography is used to investigate photochemical or photophysical parameters of molecules in a first approximation it is often possible to consider these holograms only.

Equation (3a) is the central formula for the holography described in this review. It is obvious from this equation that changes in the photochemical or photophysical properties of molecules in the holographic sample can cause changes in the diffraction efficiency η if these properties are related to corresponding changes in the index of refraction or absorbance. In the following sections of part II a new holographic method is described which measures the change of molecular parameters by following the change of the diffraction efficiency. Since, in most applications of this holographic technique, the total diffraction efficiency is small ($\eta \leq 0.01$) Eq. (3a) can be accurately approximated by Eq. (3b):

$$\eta = \left[\left(\frac{n_1 d}{\lambda' \cos\theta} \right)^2 + \left(\frac{a_1 d}{2\cos\theta} \right)^2 \right] \exp\left(- \frac{2a_0 d}{\cos\theta} \right) . \qquad (3b)$$

In these cases, η is directly proportional to the *square* of the amplitudes n_1 and a_1.

2. The Holographic Method with Continuous Wave Lasers

2.1 The detection of photochemical rate constants

If the holographic sample in Fig. 2 consists of photochemically active molecules dispersed in a polymer film or any other glassy or crystalline matrix these molecules will react in the brightly illuminated regions of the sample but not in the dark regions. As a result, a spatial variation of the photochemical product formation occurs which changes the index of refraction and the absorbance of the sample. The change in the index of refraction can be obtained from the photochemical changes by using the Lorentz-Lorenz relation[21] which gives for the amplitude n_1 after some manipulations:[20]

$$n_1 = \frac{(n_0^2+2)^2}{6000 n_0} \sum_i R_i \, \Delta C_i(t) \tag{4a}$$

where R_i is the molar refraction and $\Delta C_i(t)$ gives the time dependent changes of the concentration at the maxima of the interference pattern. The subscript i runs over all components of the reaction. A similar formula can be obtained for the changes of the absorbance caused by a photochemical reaction

$$a_1(\lambda) = 2.30 d \sum_i e_i(\lambda) \Delta C_i \tag{4b}$$

where $e_i(\lambda)$ is the extinction coefficient of the ith component of the reactio

For a simple one-step reaction

$$A_1 \xrightarrow{k} A_2 \tag{5}$$

with the overall reaction rate k the changes of the concentrations of A_1 and A_2 with time are well known from the kinetic rate equations[22]

$$C_1(t) = C_1(0)\, e^{-kt} \tag{6a}$$

$$C_2(t) = C_1(0) - C_1(0)\, e^{-kt} \tag{6b}$$

where t equals time and $C_1(0)$ is the initial concentration of A_1. Considering a pure phase hologram and putting Eqs. (6) in (4a) and (4a) in (3) gives a relationship for the efficiency as a function of time.[20,23-26] For the early stages of the hologram formation, where η is very low, Eq. (3b) can be used instead of Eq. (3a) giving the simple result:

$$\eta = (F \cdot C \cdot k)^2 t^2 . \tag{7}$$

In Eq. (7)

$$F = \frac{\pi d}{\lambda' \cos\theta} \qquad \text{and} \qquad C = \frac{(n_0^2+2)^2}{6000 n_0} (R_2-R_1)C_1(0)$$

are constants representing geometrical and material specific parameters. From an experimental observation of η as a function of time it can thus be seen that one can obtain the overall rate constant k. Curves showing η as a function of time are called hologram growth curves. The remainder of this section will indicate how one can obtain important information about photochemical and photophysical processes from such curves.

2.2 The Experimental Set-up for the Observation of Hologram Growth Curves

Experimentally hologram growth curves are obtained with an apparatus[20,23-26] similar to the one shown in Fig. 3. The light from a laser is split into reference and object waves which produce the interference pattern at the sample. The formation of the hologram can be observed in two ways. First the light from a second laser (most conveniently a HeNe laser) can be used to read the hologram. If the light of this second laser strikes the sample with the intensity I_0 it will be diffracted by the hologram. The intensity I of the diffracted beam can be chopped, measured with a photodiode and recorded with a lock-in amplifier. It is directly proportional to the diffraction efficiency $\eta = I/I_R$ and provides a record of the hologram growth as a function of time. If one chooses the wavelength of this second laser so that it is not absorbed by the sample a pure phase hologram is observed. It has to be mentioned, however, that in cases where the reading wavelength differs from the writing wavelength a different angle of incidence θ' for the reading beam must be used for the maximum intensity I. This angle should satisfy the Bragg relation[3]

$$2\Lambda \sin\theta' = \lambda' . \qquad (8)$$

For the observation of hologram growth curves relation (8) is not critical and some deviation from the Bragg condition can be tolerated. A second method of detection is to use the light of the argon laser itself. In this case a chopper is used in the object beam. When the chopper shuts the object beam only the reference wave strikes the sample. Then light of this wavelength is deflected into the direction of the object wave as the hologram grows and can be detected with a photodiode which is connected to a boxcar integrator. The reference of the chopper opens the gate of the signal input of the boxcar integrator only during the periods when the object beam is blocked so that hologram growth (open period of the chopper) and hologram detection (closed period) follow each other at the frequency of the chopper. In this way the Bragg relation is automatically satisfied.

The setup in Fig. 3 illustrates several advantages of the holographic technique. It is truly a zero background technique. Until the hologram begins to form no light is received at the photodiode. If one uses a HeNe laser for detecting the hologram, scattered light from the writing laser can be reduced by placing a narrow band pass filter before the photodiode allowing only 632.8 nm light to reach the detection. The HeNe laser beam has very little divergence so that one can further eliminate interference from scattered light simply by moving the detector well away from the sample. With such an experimental arrangement efficiencies of less than 10^{-9} can be detected.

2.3 Analysis of Hologram Growth Curves to Obtain Quantum Yields and the Number of Mechanistically Necessary Photons

With the experimental setup described above hologram growth curves[23-26] as shown in Fig. 4 can be obtained. All curves show a quadratic time dependence in good agreement with Eq. (7). For each curve in the figure, *i.e.*, for each intensity of the hologram producing beams, an overall rate constant k can be obtained according to Eq. (7).

The dependence of the overall rate constant k on the intensity can be explained by referring to the level schemes in Fig. 5. On the left side of Fig. 5 a one-photon two-level process is shown. Here the absorption of one photon excites the molecule into the reactive state A_1^*. The right side of Fig. 5 illustrates a two-photon four-level scheme indicating that two photons are necessary to reach the reactive state A_2^*. Since the rate constant k obtained above describes only the overall reaction process ($A_1 \xrightarrow{k} A_2$ for the left side or $A_1 \xrightarrow{k} A_3$ for the right side of Fig. 5), it involves the intensity dependent absorption rates I_a. In the steady state approximation it can be easily shown that k is related to the intensity I according to

$$k = \xi I^r \tag{9}$$

where r gives the number of mechanistically necessary photons and ξ contains all other photochemical and photophysical constants. For the one-photon process (r=1) in Fig. 5 one gets[23]

$$\xi = 2303 \cdot \varepsilon_1 \phi_p \tag{10a}$$

with ε_1 the extinction coefficient and ϕ_p the photochemical quantum yield, whereas for the two-photon process (r=2)

$$\xi = (2303)^2 \cdot \varepsilon_1 \varepsilon_2 \tau_2 \phi_2 \phi_p \tag{10b}$$

with ε_1, ε_2 the extinction coefficients of the two absorption steps, τ_2 the lifetime and ϕ_2 the quantum yield for population of state A_2. ϕ_p is the photochemcial quantum yield.

A plot of log k as a function of log I gives r as the slope and log ξ as the intercept according to Eq. (9). Such a plot is shown in Fig. 6 for the holographically observed photoreaction of o-nitrobenzaldehyde (ONB)[27,28] dissolved in a polymethylmethacrylate

(PMMA) film.[25] Since r=1.04 the use of Eq. (10a) with the easily obtained value of ε_1 gives the photochemical quantum yield $\phi_p=0.17\pm0.05$ for this reaction in very good agreement with the value determined by optical absorption spectroscopy. Thus the holographic method provides information about the overall photochemical reaction scheme (see Fig. 5) through the value of r, and provides information about the ratio between the rates of excited state photochemistry and photophysical relaxation processes through ϕ_p. In Sec. 2.6 the advantages of the holographic technique are discussed in more detail, however, it is already obvious from this example that important parameters such as r and ϕ can be obtained quite easily by this technique.

Several other reactions have been investigated using the holographic technique sketched above. In the field of ketone photochemistry, hydrogen abstraction by benzophenone in a PMMA matrix has been studied.[29] It has been shown that a two-photon consecutive reaction is the major pathway in the solid (see also Sec. 2.4) in contrast to solution where this pathway is a minor one.[30-32] The reaction steps involve two photons probably because of a cage effect in the solid matrix.[29,33] Another example is the holographic investigation of dimethyl-s-tetrazine[23,24,34] which dissociates in a two-photon reaction.[35,36] A so far unidentified intermediate plays an important part in this reaction. There have been several attempts to characterize this intermediate.[37-39] The holographic method has shown[34] that the intermediate which is responsible for the two-photon nature of the reaction has an absorption in the same range as dimethyl-s-tetrazine itself (see also Sec. 2.5).

2.4 Computer Modelling of Hologram Growth Curves

Hologram growth curves can have different shapes[20,29] according to the reaction mechanism underlying the production of the hologram. It is instructive to compare calculated hologram growth curves with experimentally obtained ones. One can obtain valuable

information about reaction mechanisms in this way. The basis for such a calculation is Eqs. (3) and (4). Since these equations connect the time-dependent change of the concentrations $\Delta C_i(t)$ of each component of the reaction with the hologram efficiency η the hologram growth curves can be calculated for all types of kinetic rate equations. Therefore, having an expression for the kinetic rate equations of a special reaction scheme, the appropriate growth curve can, in principle, be simulated.

Figure 7 shows such calculated hologram growth curves for first and second order holograms of a simple one-step reaction $A_1 \xrightarrow{k} A_2$ as in Eq. (5).[20] The second order hologram can be observed at an angle 2θ. It is weaker than the first order hologram and results primarily from the fact that after prolonged irradiation times the change of the index of refraction reaches saturation due to bleaching of the photoactive material in the bright parts of the interference pattern. This can be seen in Fig. 8 where the change of the index of refraction is calculated for increasing reaction times. As a result of the bleaching process, n(x) must be described by a Fourier expansion for longer reaction times instead of the simple two term expression in Eq. (2). Higher order holograms are then due to higher order coefficients of n(x) in the Fourier expansion.

The experimentally observed curves in Fig. 4 for a one-step reaction are obtained only for the very first part of hologram growth well before saturation begins. If one expands the timescale in Fig. 7, a clear quadratic time dependence is found for the early stages of hologram growth as observed experimentally and described by Eq. (7).

Hologram growth curves can be calculated for more complex kinetic schemes. For example, a consecutive reaction

$$A_1 \xrightarrow{k_1} A_2 \xrightarrow{k_2} A_3 \qquad (11)$$

has been treated. Results for such a calculation are shown in Fig. 9. For the reaction scheme outlined in Eq. (11), one can, according to Eq. (4a), write

$$n_1 \propto \Delta C_2 R_2 + \Delta C_3 R_3 - (\Delta C_2 + \Delta C_3) R_1 \, . \tag{12}$$

For the case shown in Fig. 9b, $R_1 > R_2 > R_3$. n_1 is thus negative throughout the reaction. In this case we expect the hologram to grow initially at a rate characteristic of the $A_1 \rightarrow A_2$ reaction but eventually to grow with the $A_2 \rightarrow A_3$ rate. This is exactly what occurs in Fig. 9b.

If, perhaps in another wavelength region, $R_2 > R_1 > R_3$ the result in Fig. 9a is obtained. During the initial stage of the reaction while A_1 is being converted to A_2, the hologram grows at a rate characteristic of this reaction. But as the reaction proceeds further A_2 is replaced by A_3 and since $R_3 < R_1$ this means that n_1 must eventually become negative. Following n_1 as a function of time, we find that n_1 begins to decrease during the second phase of the photochemistry passing through zero and eventually becoming negative. Since the hologram efficiency depends on the square of the quantity n_1, the expected hologram growth pattern is shown in Fig. 9a.

Such hologram growth curves have been observed for the consecutive photoreaction scheme of benzophenone in PMMA.[20,29] Results at two different wavelengths corresponding to the two cases discussed above are shown in Fig. 10.

These examples show that characteristic shapes of hologram growth curves occur for different types of reactions. As long as expressions for the kinetic rate equations are available these shapes can be calculated and compared to the experimentally observed features. In this way they can help to prove the underlying reaction mechanism.

2.5 Observation of a Photochemical Action Spectrum Using Holography

As a final example of the use of the cw holographic technique in photochemical investigations the observation of a photochemical action spectrum will be discussed.[29,34,40] Many examples exist of photochemistry that occurs when a molecule in its lowest metastable triplet state is excited to a higher triplet state.[41] The holographic technique is particularly useful for studying such processes because it can be used even in cases where interfering reactions occur from the lowest triplet state.

To illustrate the use of holography in this context, we consider the first step in the benzophenone hydrogen abstraction process.[29] As discussed in Sec. 2.3, this process involves the consecutive absorption of two photons. The first photon at a frequency ω_2 excites the $S_0 \rightarrow S_1$ absorption as shown in Fig. 11. After intersystem crossing the lowest triplet state T_1 is produced. Absorption of a second photon at ω_1 produces T_3. As a result of photochemistry undergone by T_3, a product known as the light absorbing transient (LAT) is produced.

The question arises as to which excited states are responsible for the photochemical reaction, T_3 itself or an intermediate triplet state T_2 that is reached by radiationless relaxation from T_3. The holographic technique is ideally suited to answer questions like this. Figure 12 indicates how this might be done. A UV source that need not be coherent excites the benzophenone molecules at ω_1 ultimately producing molecules in the T_1 state. Note that even if this irradiation results in photochemistry no hologram is produced since there is no interference pattern.

If two interfering beams at a frequency ω_2 now strike the sample, they can excite the benzophenone molecules to a higher triplet state. If photochemistry occurs from this higher

state, then a hologram will be formed. By varying the frequency ω_2 and following the hologram growth rate, a photochemical action spectrum may be obtained. For benzophenone these results indicate that, referring to Fig. 11, the $n\pi^*$ state T_3 is reactive, but the $\pi\pi^*$ T_2 is not.

Investigations using this technique have also been performed for the N-H bond cleavage reaction of carbazole[40a] and the previously discussed photodissociation of dimethyl-s-tetrazine.[34]

2.6 Comparison of the cw-Holographic Method With Conventional Absorption Spectroscopy

After these examples of the application of cw holography to determine photochemical parameters it seems useful to compare the method with other spectroscopic methods, such as optical absorption spectroscopy. The holographic method is sensitive to changes in both the index of refraction and absorption coefficient. Thus, this holographic technique encompasses both dispersion and absorption spectroscopy. To illustrate this important point, Fig. 13 shows the absorption curve $\varepsilon(\lambda)$ and the related dispersion curve $n(\lambda)$ for an optical transition with a maximum at the wavelength λ_0. Both quantities are connected by the Kramers-Kronig relation[42] and can be calculated from each other. Therefore, in principle, the dispersion curve in Fig. 13 does not contain any new information about the molecule as compared to the absorption curve. However, differences do exist between spectroscopic absorption and dispersion techniques.

So, for example, it is obvious from Fig. 13 that the detection wavelength for the observation of a photochemical reaction by absorption is restricted to the wavelength range of absorption whereas observation by dispersion can also be done outside the absorption region. Since the holographic technique most frequently involves phase holograms one has a

free choice for the detection wavelength. This has the advantage that overlapping absorption bands do not prevent the investigation of the kinetics of a reaction, and that complicated reaction schemes (*e.g.*, A→B→C) can be observed at one wavelength without interrupt even when the reaction compounds have totally different absorption spectra. Further, the detection wavelength can be chosen in a spectral range where the detection system has high sensitivity or where convenient laser sources are available.

Since for a pure phase hologram the detection beam is *not* absorbed one has the additional advantage of being able to choose the intensity of the detection beam. Using very high power in this beam does not destroy the sample but can give improved sensitivity. In contrast to conventional optical absorption spectroscopy high sensitivity of the holographic technique is also obtained, as previously mentioned from the fact that the hologram grows out of the dark, *i.e.*, the holographic method is a zero-background technique.

From Eqs. (3) and (4a) it can be shown that the sensitivity of the holographic method in dispersion should be as high as that of a method involving optical absorption. At first sight this seems astonishing since the range of the index of refraction n for organic molecules, for example, is very small. This small range for n also explains why there exists few useful techniques that rely on dispersion (an exception is optical rotatory dispersion spectroscopy[43] for optically active materials).

In fact the holographic technique is by far the most sensitive method for measuring small changes in the index of refraction. A 0.1% change in n can result in a diffraction efficiency of 80% or more. Thus, the holographic technique outlined in this paper adds an optical dispersion method comparable in sensitivity to and complementary with optical absorption spectroscopy.

3. The Holographic Method with Pulsed Lasers (Transient Gratings)

3.1 Creation and Detection of Transient Gratings

Lasers can be run not only in the continuous wave (cw) mode, but can also be used as pulsed light sources giving very short light pulses with a pulsewidth ranging from about a picosecond up to several nanoseconds.[44] These pulses can be selected as single pulses out of a pulse train or can be obtained at a high repetition rate. If such a laser pulse is split by a beamsplitter, as indicated in Fig. 3, then provided the path lengths are equal two laser pulses arrive at the sample coincident in time but from different directions. Because both pulses originate from the same laser and are thus coherent, an interference pattern is created at the sample which exists for a duration approximately equal to the pulsewidth. Due to photochemical or photophysical processes involving the molecules in the sample, a holographic grating is induced quasi-instantaneously. After the pulses have left the sample, this grating may decay because of relaxation processes in the sample.

This decay can easily be observed by using a probe pulse with variable time delay. The probe pulse will be diffracted by the grating and its diffracted intensity as a function of delay time will give the time dependent decay of the grating. An experimental setup[45-47] with pulsed lasers can be run at a high repetition rate (*e.g.* 500 Hz) measuring the diffracted probe pulse intensity averaged over many pulses, while slowly varying the time delay between excitation and probe pulses. The time resolution of such an apparatus is given approximately by the pulsewidth of the laser pulses. The decay of such a grating can, of course, also be observed by a diffracted cw-detection beam whose time dependent intensity shows the decay of the grating. Since the above described holographic grating exists only for a short period of time the holographic method using pulsed lasers is often called the transient grating technique.[45-49]

Unlike the cw-holographic method, the transient grating technique is not restricted to investigations of molecules in the solid state but can also be used for molecules in the liquid phase. A wide variety of time dependent phenomena can be observed by this technique. Examples include processes like the relaxation of excited states[50,51] photoreactions from excited states,[52] energy transfer across the fringe pattern,[53] energy trapping,[54] diffusion processes of molecules,[45,51] carrier transport in semiconductors,[46,55] optical generation and detection of ultrasonic waves,[47] and thermal diffusion.[49] In the following sections, we will concentrate on a few examples of the technique.

3.2 Excited State Dynamics: Lifetimes, Photoreactions and Energy Transfer

In this section, we want to concentrate on transient gratings produced by time dependent phenomena involving excited states of molecules excluding any effect which may result from the diffusion of the molecules themselves. Thus, we are first restricting our discussion to transient grating effects involving molecules in the solid state or where the relaxation times of interest are much shorter than any observable molecular diffusion process. We will discuss three cases dealing with lifetimes of excited states, photoreactions and energy transfer.

If molecules in the holographic sample are excited by two interfering laser pulses to higher electronic or vibrational states, their index of refraction or absorbance will change because of rearrangements in the electronic structure of the molecules.[56] Thus, a holographic grating will be produced in the same general manner as discussed in Section 2. Since the change of the index of refraction or absorbance is proportional to the number of molecules excited, the diffraction efficiency η depends on (N_1),^{2} *i.e.*, the square of the number of the excited states at the grating peaks. Here, the simple Eq. (3b) has been used because of the low hologram efficiency produced by the excited states. In the absence of

any other processes besides the relaxation of the excited states to the ground state, the time dependent intensity I(t) of a diffracted probe beam will be determined by the excited state lifetime τ:

$$I(t) = A \exp\left(-\frac{2}{\tau} t\right) . \tag{12}$$

In Eq. (12), A is a constant gathering together all time independent holographic parameters and the factor two in the exponential expression arises because of the quadratic dependence of the signal intensity I(t) on $N_1(t)$. A logarithmic plot of log I(t) against time t will give the decay rate $k=2/\tau$ as the slope and A as the intercept. Thus, lifetimes of excited states can be obtained easily with the transient grating technique.[45,50] This can be important for states that decay without the emission of radiation and which cannot thus be investigated by optical emission techniques. Further from the value of A in Eq. (12), the differences of the molar refractions of the ground and excited states can be elucidated. This gives the possibility in principal of determining polarizabilities of excited molecules.[57]

Besides the radiationless or radiative relaxation of excited states, a photoreaction can also occur from these transient states as discussed in Section 2. It is of interest to see if any complementary information can be obtained by the transient grating technique that cannot be obtained by the cw-holographic method. Without going into details and restricting ourselves to the simple case of a one-photon two-level reaction scheme (see Fig. 5), it can be shown that the time dependence of the diffraction efficiency should be given by[52]

$$\eta(t) = K_1 + K_2 \exp - (k_1 + k_2)t . \tag{13}$$

In this equation, K_1 and K_2 are time independent constant whereas k_1 and k_2 are rate constants for the decay of the excited state and the photochemical step respectively as indicated in Fig. 5. Assuming that the population in the excited state is established

instantaneously by the two interfering laser pulses, k_1 describes the decay of the transient grating while k_2 characterizes the time dependent increase of the modulation depth of the grating due to the creation of photochemical products. Thus, in this case, a photophysical hologram decays and a photochemical hologram grows. The rate constants for both processes can be obtained from the experimental measurements with the following procedure: First the final value of $\sqrt{\eta(t\to\infty)}$ is determined for a time t after the exciting laser pulses which is long compared to $1/(k_1+k_2)$. Then a plot of $\ln [\sqrt{\eta(t)} - \sqrt{\eta(t\to\infty)}]$ against time will give (k_1+k_2) as the slope. If this result is *combined* with the photochemical quantum yield $\phi_p = k_2/(k_1+k_2)$ obtained from the cw-holographic experiment the lifetime of the excited state $\tau = 1/k_2$ and the rate constant k_1 of the photochemical step can be determined. Thus, a combination of both cw and pulsed holographic methods can provide a detailed picture of the photochemical reaction. It is also possible to obtain k_1 and k_2 from the application of one of the holographic methods and a spectroscopic lifetime measurement.

Starting again from the modulated pattern of excited states created by two interfering laser pulses, as a third example, one can describe the subsequent dynamics of an excited state not only by radiative and radiationless relaxation to the ground state but also by energy transfer[58,59] to neighboring molecules. For these processes, molecular crystals[60] provide an important example. Their energy transfer has been studied at least in part as a model for energy transfer in biological systems.[61,62] In molecular crystals, energy transfer results from intermolecular interactions and can be thought of as a migration of an excited state by hopping from molecule to molecule in the time before relaxation to the ground state. Because intermolecular interactions are anisotropic, the rate of energy transfer is often easier along some crystallographic directions than others. If a transient grating is created in such a crystal, its decay will thus depend on two processes: First the excited state lifetime τ will

reduce the amplitude of the fringe pattern as discussed above and second, the migration of the excited states perpendicular to the fringes will wash out the modulation pattern. Assuming that the energy transport can be described as a diffusion process with a diffusion constant D, the observed signal intensity I(t) of the diffracted probe beam should show an exponential decay as in Eq. (12), however, the decay rate k must be modified by a second term describing the diffusion process:[53]

$$k = 2/\tau + (8\pi^2 D/\lambda^2)\theta^2 . \qquad (14)$$

Since the effect of the diffusion process on the overall decay depends on D and in addition on the fringe spacing Λ (see Eq. (1)), the second term in Eq. (14) depends on λ and θ. Performing transient grating experiments with different fringe spacing, *i.e.*, by varying θ, a set of decay constants k can be measured. From the slope of a plot of k as a function of θ^2, the diffusion constant D can be calculated, whereas the intercept of the plot yields the lifetime τ. Thus, transient grating experiments with variable fringe distances are capable of separating lifetime and diffusion effects quite easily.

Such measurements have been done by several workers.[46,50,53,63] In Fig. 14, the results of Siegman and Fayer *et al.*[53] are shown. They investigated a single crystal of p-terphenyl doped with 10^{-3} mol/mol of pentacene. Obtaining k from decay curves as in Fig. 14a and plotting k as a function of θ^2 (see Fig. 14b), they obtained a diffusion constant $D=2\pm0.1$ cm^2/s for the energy transfer along the crystallographic b axis. The intercept $2/\tau$ was in good agreement with the independently measured lifetime $\tau=9.5\pm0.3$ nsec. Since such measurements can be done along different crystallographic directions by simply rotating the holographic sample the anisotropy of energy transfer and thus of intermolecular interactions can be studied in a very direct manner.

It should be emphasized that the transient grating technique with variable fringe distances is not just restricted to diffusion by energy transfer. In principle, any diffusive process that reduces the peaks and fills the nulls of the modulation pattern can be investigated. So, for example, transient gratings have been produced in *semiconductors.*[46,55,64] In these materials, the gratings are due to the formation of free carriers and the decay of the grating gives the characteristic diffusion constant for the movement of the free carriers. Other systems in which light induced charge transport is of great importance include *electro-optic crystals* such as $LiNbO_3$ and $LiTaO_3$ doped with transition metals. These materials have been considered as potential candidates for holographic information storage[16] and have a variety of other applications in modern optics. The photoinduced electron and hole transport in these materials has been investigated by holographic methods.[65] So far, mainly cw-holographic methods have been used,[66] however, the transient grating method would also seem to be suitable.

The holographic technique can be used to measure the chain length of polymers. For example, the photopolymerization of diacetylene single crystals has recently been observed with a holographic setup.[67] The disappearance of the hologram due to the growth of polymeric chains across the fringe pattern was investigated. So far, the chain length did not exceed the spatial resolution of the holographic grating so that only an upper limit on chain length could be determined. These investigations have been done using a cw holographic technique but could also have been done with the transient grating technique.[57]

3.3 Rotational and Translational Diffusion Processes in Liquid Solutions

In the sections above, it was assumed that the molecules under investigation had fixed positions relative to the polarization of the exciting as well as the detecting light pulses because they were incorporated in an ordered or unordered way in a crystalline or glassy

matrix. However, if the experiments are performed in liquid solution, the molecules can diffuse within the sample showing rotational as well as translational diffusion. Since laser light is linearly polarized, the two interfering light pulses will preferentially excite molecules with a transition moment parallel to the electric vector of the light waves. So not only a spatial modulation pattern of excited states is created by the interference of the two light pulses but also a selection of preferentially oriented molecules. For these molecules in a liquid solution, it is possible to follow rotational diffusion if the polarization of the delayed probe pulses relative to the exciting laser pulses is taken into account.[51] Since rotation of molecules in solution will occur much faster than noticeable diffusion of excited molecules from the peaks into the nulls of the grating, it is the rotational and not the translational diffusion which is observed first using linearly polarized laser light as a probe beam. As in time resolved fluorescence depolarization experiments[68,69] the decay of the transient grating is measured with two time dependent signals[51] $I_{\parallel}(t)$ and $I_{\perp}(t)$ which are obtained for parallel or perpendicular orientation of the probe pulse relative to the excitation pulses. A detailed analysis[51,70] of the time dependence of the signals $I_{\parallel}(t)$ and $I_{\perp}(t)$ shows that the sum S(t) of both signals gives an exponential decay with a decay constant $k=1/\tau$ where τ is the lifetime of the excited state. Computing the difference D(T) of both signals $I_{\parallel}(t)$ and $I_{\perp}(t)$ and taking the ratio $R(t)=D(t)/S(t)$ it can be shown that R(t) gives an exponential decay too, however, the decay constant $k_R=1/\tau_R$ yields the rotational reorientation time τ_R. So, by performing two time dependent measurements, $I_{\parallel}(t)$ and $I_{\perp}(t)$, it is possible to *separate* the lifetime effect from the reorientation of the molecules.

In Fig. 15a, the two time-dependent signals $I_{\parallel}(t)$ and $I_{\perp}(t)$ are shown for a sample of Rhodamine B in n-propanol as obtained by Fayer *et al.*[51] Figure 15b shows the

corresponding logarithmic plot of S(t) and R(t) giving the excited state lifetime τ and the rotational reorientation time τ_R, respectively.

It is interesting to note that the above obtained excited state lifetime can be checked in a third experiment. Setting the polarization of the probe beam at 54.7°, (the "magic angle") relative to the excitation polarization, it can be shown that the observed decay is independent of rotational dynamics. In this case, the exponential decay of the signal $I_M(t)$ gives directly the excited state lifetime τ. So both independently obtained values for τ can be compared.[51]

In principle, this last experiment using the "magic angle" of 54.7° is well suited for an investigation of translation diffusion processes in liquids since it eliminates the rotational diffusion effects on the signal. A combination of a "magic angle" experiment with a variation of the fringe distance Λ by changing the angle of incidence θ as described for the energy transfer process in Section 3.2 should give the translational diffusion constant of molecules in solution. However, for such an experiment, the lifetime of the excited states of molecules has to be in the range of the diffusion time necessary to give noticeable equilibration between the peaks and the nulls of the grating. For the above mentioned investigation of Rhodamine B dissolved in n-alcohols or photoproducts with lifetimes that are sufficiently long, the translational diffusion of the photoproducts from the peaks to the nulls of the grating can be observed. In this case, a combination of time dependent experiments with the variation of the angle of incidence θ can give the translational diffusion constant for the photoproducts in solution. Experiments of this kind are currently in progress.[71]

The investigation of rotational reorientation and translation diffusion of molecules in liquid solvents can be used to probe solute conformations, solvent-solute interactions and local solvent structure.[68,74] In particular, the predictions of the Debye-Stokes-Einstein

hydrodynamic theory[75] can be examined yielding the effective volume of the rotating molecule as a characteristic parameter. So far, such investigations have been done by applying time resolved absorption[76] or fluorescence depolarization spectroscopy[68,69] in the picosecond time regime. With the transient grating technique, an additional technique is available. Since this technique is a dispersion technique, "saturation effects" for τ_R plotted as a function of viscosity found earlier[69] are not observed with the transient grating technique as expected from theoretical calculations.[51] Further, the transient grating method measures rotational reorientations τ_R of molecules in the excited and the ground state whereas fluorescence depolarization experiments examines *only* the excited state rotation. Thus, combining both methods can provide a measure of the differences in the excited and ground state rotation times. A preliminary estimation[51] gives differences of up to 30%.

3.4 Energy Transfer and Trapping in Liquid Solutions

Energy transfer in liquids is related to the problems discussed in the previous section. Theoretical calculations[77] have shown that at very high concentrations, the excited state transport in liquids should occur as a rapid diffusion over macroscopic distances, comparable to the fringe spacing of the transient grating. However, experimentally, this has not been observed[54] because the time dependence of the diffracted signal was not correlated to a variation of the fringe spacing of the grating. Using rhodamine 6G (R6G) in glycerol and ethanol as solute/solvent systems, it was found that an increase of the concentration of R6G leads to a trapping of the excited state energy by dimers instead of long range energy transfer. For high concentrations of R6G, it has to be assumed that ground state dimers are formed[78] which have distinct spectral properties. Although the energy transfer among the monomers becomes more efficient at high concentrations, the possibility of finding a dimer and of being trapped increases also. When an excited state is trapped on a dimer, a fast

radiationless relaxation to the ground state occurs indicated by fluorescence quenching.[79] The fast radiationless relaxation rates of dimers can be understood because of the loose complex nature of the dimers which allows rapid configurational changes. So, energy transport over macroscopic distances in liquid solutions could be ruled out by the transient grating technique. Further, by setting up rate equations for the time dependent signals of the transient grating based on the model of energy trapping as discussed above, the decay rates of the monomers and the excited dimers to the ground state as well as the trapping rate for the excited state energy transfer could be determined. The trapping rate is proportional to the cube of the concentration of R6G.[54] This is an important result for *e.g.*, dye laser technology because concentration quenching of excited states is an important effect limiting the gain of such systems.

3.5 Optical Generation of Ultrasonic Waves by Transient Gratings

So far, local heating by the absorption of the two interfering light pulses has not been taken into account. With moderate laser power, this effect is negligible. However, if high laser power is concentrated in short laser pulses considerable heating can occur in the sample.[46,47,80-82] Since this heating is due to radiationless relaxation processes of the excited molecules, it is concentrated at the local maxima of the transient interference pattern and causes a thermal expansion in this region of the sample. Thus, the density in the peaks of the grating is reduced whereas the density in the nulls is increased. As a result, a counterpropagating density wave (a standing density wave) is created, which is present even after the two exciting pulses have left the sample. In this way, an ultrasonic wave can be generated optically in the medium. It is obvious that the wavelength of this wave is determined by the fringe distance Λ. Since Λ can be varied easily, in a broad range from

about 1 mm to 0.1 μ, tunable acoustic frequencies from about 3 MHz to 3 GHz can be generated by simply changing the angle of incidence θ.[47]

Since the oscillating density changes of the ultrasonic wave cause oscillations of the amplitude n_1 of the index of refraction, the ultrasonic wave can be detected with diffracted time delayed probe pulses in the ordinary manner. Results are shown in Fig. 16c for a $5 \cdot 10^{-5}$m solution of malachite green in ethanol,[47] where the excitation wavelength was chosen in the absorption region of malachite green.

Another mechanism for generating ultrasonic waves by transient gratings uses stimulated Brillouin Scattering instead of absorption.[83,84] This mechanism is similar to stimulated Raman scattering. A higher frequency photon in one of the two interfering beams is cancelled and a lower-frequency photon in the other beam is created. The result is an acoustic phonon with a frequency equal to the difference of the frequencies of the two photons. In addition to the conservation of energy, the conservation of momentum has to be satisfied. The spread in frequency in the two interfering pulses is always broad enough to allow efficient phonon generation at any angle of intersection of the two interfering beams. It has to be emphasized that in this mechanism, no absorption and therefore no heating occurs. There is a direct coupling of the optical electromagnetic field to the material acoustic field. Thus, this effect can be observed without absorption of the interfering beams as shown in Fig. 16a for a solution of pure ethanol.[47] A more detailed description[47,82,84] of the heating effect and the stimulated Brillouin scattering shows that different time dependences of the diffracted signal arise which allow a separation of the two mechanisms. In Fig. 16b, an intermediate case is shown where both mechanisms are visible because of the very low concentration of malachite green.[47] Both of the above mentioned mechanisms have to be

taken into account when decaying signals of transient gratings as described in the foregoing sections show an oscillating behavior.[53,80,82,84]

Since the ultrasonic waves can be optically generated in liquids and in solids, there are a wide variety of applications.[46,47] The technique can be used for nondestructive acoustic testing of materials, for measuring anisotropic elastic constants, acoustic attenuation, isotropic and anisotropic thermal diffusion, photoelastic constants and a variety of other interesting material parameters.

III. NEW MATERIALS FOR HOLOGRAPHY

1. Holographic Materials

In the preceding discussion we have shown how the development and decay of a hologram can be used to obtain information on a variety of physical and chemical processes. We will now turn this approach around and show how these studies of solid state chemistry can result in the development of new classes of holographic recording materials.

A variety of materials have been considered for holographic recording. Table I lists a few of these materials and the subject has been treated in a number of reviews.[85,86] One can list several desirable criteria for holographic materials. A reasonably high efficiency is desirable, but efficiencies approaching 100% are not necessary. The photosensitivity should be high, *i.e.*, the time required to reach maximum efficiency should be as short as possible. The recording material should be sensitive in wavelength regions accessible to commercially available lasers. The hologram must not be erased during reading so some method of fixing the recorded interference pattern is necessary.

Table I illustrates the point that no material satisfies all of these requirements. On the other hand, a material-like dichromated gelatin is perfectly adequate for many applications and has proven quite useful.[87]

One severe limitation in all of the currently available materials is their spectral sensitivity. This sharply limits the number of possible laser sources that can be used directly. Dichromated gelatin, for example, cannot be used at wavelengths longer than 500 nm.[87] Responses to wavelengths as long as 748 nm have been obtained using photographic film such as Kodak 649F or 120-01.[88] Attempts to spectrally sensitize dichromated gelatin or holographic quality photographic film to longer wavelengths have so far produced unsatisfactory results. At present no single-photon volume holographic recording material with response at wavelengths longer than 750 nm exists. This is unfortunate because it means that there are no holographic materials compatible with the convenient and inexpensive injection diode laser such as GaAlAs (800-850 nm) or GaInAsP (1.2-1.6 μm).

As a result of some of the photochemical investigations described in the first part of this paper, a new technique has been developed involving *two-photon four-level photochemistry* for the production of holograms in the red and infrared.[89,90] In addition to their spectral sensitivity, these materials have the advantage that they are self-developing and require no fixing step. Furthermore, the hologram can be gated off and on by utilizing an auxiliary light source.

2. Two-Photon Four-Level Photochemistry

Most holographic recording materials utilize photochemical reactions in which the rate of product formation depends linearly on laser light intensity. Such a scheme is shown at the left of Fig. 5. Only two levels of the molecule A_1 are involved in the photochemistry. It

can be shown[23] that the overall rate constant k for product formation is proportional to the molar extinction coefficient ϵ and is linear in laser intensity I as previously indicated:

$$k \propto \epsilon I . \tag{15}$$

Now consider using such a two-level medium for holographic recording. Such an experiment is shown schematically in Fig. 1. Normally the reconstruction wave will be at the same wavelength as the object and reference waves. This means that the reconstruction wave itself can also produce photochemistry. This photochemistry will result in gradual erasure of the hologram. There are two ways of eliminating or minimizing the effect of erasure during reading for one-photon materials. The first, and less satisfactory method, is simply to reduce the reading light intensity so that the photochemistry that occurs during reading is reduced to an acceptable level. This is, of course, impractical when the hologram is meant to be semi-permanent. The most commonly used method of eliminating erasure is to fix the holographic image permanently. This is done in dichromated gelatin and silver halide films by wet chemical processes.

Another disadvantage of one-photon materials arises when one considers extending their sensitivity into the red and infrared regions. All of the energy used to produce photochemistry must come from the absorbed photons. Very few systems undergo efficient photochemistry in the red or infrared, and those few systems that do also tend to be thermally unstable. This point is illustrated in Table II where laser wavelengths and bond energies are compared. Both AIBN and hexamethylethane shown in the table are thermally unstable.

It has been recognized by previous workers that many of the problems with the one-photon systems are either not present or are significantly reduced in importance when

the hologram forming photochemical process involves the absorption of two or more photons.[91,92] These investigators employed a two-photon three-level system. The energy level diagram for such a system is similar to the four level scheme shown in Fig. 5 with the difference that A_1^* and A_2 have now been combined into a single level. In a three-level system, the recording medium is simultaneously exposed to radiation at two different optical frequencies ω_1 and ω_2 with intensities I_1 and I_2. The rate constant k for product formation is now given by

$$k \propto \epsilon_1 I_1 \epsilon_2 I_2 \tau \tag{15}$$

where ϵ_1 and ϵ_2 are the respective molar extinction coefficients at the two frequencies ω_1 and ω_2. τ is the lifetime of the intermediate state.

Consider the simple case where $\omega_1 = \omega_2$. The photochemistry is then proportional to I_1^2. Any reduction in the laser intensity during reading would have its effect on hologram erasure reduced by the square of this factor. In addition the energy to produce photochemistry is now supplied by two laser photons and it should not be difficult to find thermally stable two-photon systems that could be used with red or infrared radiation.

Perhaps a more interesting case is when $\omega_1 > \omega_2$. The medium is illuminated by reference and object beams at a frequency ω_2, as well as by an additional uniform and not necessarily coherent beam at ω_1. Note that we have treated this case in another context in the discussion associated with Fig. 12. Holograms formed using this approach have several advantageous properties. As for the case where $\omega_1 = \omega_2$, these materials can be written with red or infrared lasers. Most of the energy needed to produce photochemistry is supplied by the ω_1 photon which can be in the ultraviolet. Another important advantage is that the recording medium is sensitive to the ω_2 radiation only when ω_1 radiation is present. Thus,

during the reconstruction of the image for readout no additional deleterious exposure of the recording medium takes place. Also, temporal or spatial gating of the recording can be achieved by masking or modulating the ω_1 beam.

The first demonstrations of two-photon holographic recording were in $LiNbO_3$ and KTN ($KTa_xNb_{1-x}O_3$), where the recording process was the multi-photon photorefractive effect.[91,92] This effect involves the excitation of carriers within the crystal lattice to produce a macroscopic polarization change that induces a modulation of the index of refraction via the electro-optic effect. The major disadvantage of these materials is the lack of real intermediate energy levels between the ground and final states. Since the resonant enhancement from these intermediate levels is not present, the two-photon absorption processes are extremely weak and peak exposure intensities greater than 5 MW/cm^2 are necessary. A factor of 100 improvement in sensitivity was demonstrated by doping the $LiNbO_3$ crystal with Cr^{+3}, thereby converting the intermediate level from a virtual to a real level with a 500 ns lifetime.[93] The resulting sensitivity, however, was still several orders of magnitude too low for cw two-photon holography.

It can be shown[90] that no three-level system can be sensitive enough to be used for holographic recording with cw lasers. This can be seen qualitatively by considering the role played by the intermediate state. For optimum production of photochemical products one wants the population in this state to be as large as possible. This means that the extinction coefficient ϵ_1 should be large and the lifetime τ of this state should be long. However, these two quantities are not independent since lifetime and absorption strength are related to each other. There is thus an upper limit to the rate k that one can obtain for a three-level two-photon system.

To produce two-photon holographic systems that can be used with cw laser sources, one must circumvent these constraints. One way of doing this is to use the two-photon four-level system illustrated at the right of Fig. 5. There are now two intermediate levels A_1^* and A_2. Level A_1^* may have a large oscillator strength with respect to transitions from the ground state, while level A_2 may have a long lifetime. It thus should be possible to find a two-photon four-level system with which one can produce holograms using only a few milliwatts of cw laser power.

A variety of organic materials have energy level systems arranged as shown in Fig. 5. States A_1 and A_1^* are the lowest ground state and an excited singlet state of the molecule, respectively. A_2 and A_2^* may be ground and excited states of an isomeric form of the molecule or they can be excited triplet states. In fact, such systems are described in Part III, Sec. 2.5. In that earlier discussion we were interested in using holography to investigate excited state photochemistry. Here we note that benzophenone[29] and carbazole[89] can be used in two-photon four-level holographic recording materials.

The holographic system that has been most thoroughly investigated in this context is biacetyl dissolved in a polymer host matrix.[90] The relevant absorption spectra of biacetyl are shown in Fig. 17. The initial photon excites the biacetyl molecule from its ground state to an excited singlet state S_n. This can be done according to the figure, provided the exciting wavelength is shorter than 500 nm. The second photon produces the hologram by exciting the biacetyl from $T_1 \rightarrow T_n$. This occurs if the second wavelength is between 600 and 1100 nm. The hologram is produced as a result of a photochemical reaction that occurs from T_n.

Hologram formation in biacetyl[90] is illustrated in Fig. 18. The experimental arrangement was similar to the one sketched in Fig. 12. The matrix in which the biacetyl was dissolved for these experiments was a polycyanoacrylate polymer. Irradiation at ω_1 was provided in the UV by a medium pressure Hg-lamp. The infrared source at ω_2 was a Kr^+ laser operating at 752 nm. At time t=0 only the IR source illuminates the sample. Since this light is not absorbed by a ground state biacetyl molecule, no hologram is produced. When the UV source is turned on hologram formation begins. When it is turned off the hologram growth is gated off. Holograms formed in this way require no chemical development step. They are "developed" simply by turning off the UV source.

3. Applications of Two-Photon Materials

In this section we will illustrate several applications of four-level two-photon infrared holographic materials. The most familiar application for materials of this type is in the production of three-dimensional images. The recording of an extended image using the biacetyl/polycyanoacrylate system is shown in Fig. 19.[94] The hologram was produced and reconstructed at 752.5 nm.

The advantage of recording extended holographic images in this way lies in the possibility of spatially or temporally gating the process. By spatially gating hologram formation one can imagine the production of holographic movies with frame to frame exposures gated on and off with the UV source. Temporal gating, of course, provides the potential for recording holograms at precise well-defined instants in time.

In the future holograms will probably be most widely used for the production of a variety of kinds of optical elements for the deflection and focusing of light. Holographic optical elements (HOEs) utilize the fact that a hologram is capable of transforming a family

of incident waves. The simplest example of a HOE is the holographic grating formed by the interference of plane object and reference waves. This type of HOE was described in Sec. II where its use for monitoring photochemistry was treated. Another example is the holographic lens that is formed by the interference of a spherical object wave with a spherical or plane reference wave. Figure 20 shows the recording geometry for the production of an off-axis holographic lens. The properties and applications of HOEs have been the subject of several recent reviews.[95]

The fundamental advantage of HOEs is that a complex and expensive optical system can be replaced by a cheap and simply fabricated piece of plastic. This is a particularly important consideration when one wishes to use the HOE with an inexpensive injection diode laser.

Figure 21 illustrates the results of the production of a holographic lens in the biacetyl/polycyanoacrylate system.[94] The hologram was produced at 752.5 nm. Position 1 is near the lens focal point and Position 2 is beyond that point. One clearly sees the focusing effect of the HOE. The hologram was reconstructed at both 752.5 and 799.3 nm. It is clear in both cases that the HOE operates as a focusing element. It is also apparent, however, that the focal point is not as sharp for reconstruction at 799.3 nm. This illustrates the important point that image quality and diffraction efficiency degrade as the reconstruction wavelength departs from the wavelength of the original object and reference waves.

As a final example of the use of the infrared hologram recording technique described above, we consider the fabrication of integrated optical devices.[96] The general principal of these devices is illustrated in Fig. 22a. The two interfering infrared beams intersect inside a

narrow dielectric waveguide formed from a thin biacetyl/polycyanoacrytlate layer between glass plates. Since the infrared beams are confined within a several micron thick dielectric layer, power densities can be quite high. Input powers of a few milliwatts can result in waveguide power densities of a few kilowatts/cm^2. This is particularly important for the two-photon four-level materials that tend to have low recording sensitivities.

A hologram can be formed at the intersection between the two infrared beams and a UV beam as shown in Fig. 22a. An example of an integrated optical device fabricated in this way is the directional coupler shown in Figs. 22b and 22c.[97] In these photographs one is looking down on the glass plates from above. The infrared light that is observed is scattered from defects in the recording layer. In Fig. 22c the directional coupler is illustrated. A portion of the input beam is coupled by the device into another direction.

IV. *CONCLUDING REMARKS*

In this review we have discussed a variety of material parameters that one can study using holographic grating techniques. Excited state photochemistry, energy transfer, rotational relaxation, charge transport, polymerization, to name a few all can be conveniently studied using holography. One can use cw or pulsed versions of the technique.

It is also possible, as we have shown, to use fundamental photochemical information obtained by holographic techniques, to suggest new classes of holographic materials. This point has been illustrated by a discussion of infrared sensitive two-photon four-level holographic recording materials.

ACKNOWLEDGMENTS

Both authors would like to acknowledge fruitful collaborations with a number of co-workers whose names appear in the reference to this paper. One of the authors (DMB) is

also grateful to the Office of Naval Research and the U.S. Army Research Office for partial financial support.

Table 1

Holographic Materials

Material	Advantage	Disadvantage
dichromated gelatin	large Δn thin coatings	spectral sensitivity recording speed passivation shelf life
photopolymer	self-developing no shrinkage inert coating ease	small Δn thick coatings spectral sensitivity
photographic film	spectral sensitivity chemical amplification reproducibility	medium efficiency substrate choices resolution
photoresist	replication coating ease stability	spectral sensitivity recording speed linearity
thermoplastic	self-developing high sensitivity erasibility	spectral sensitivity efficiency resolution

Table 2

Energy and related wavelengths of various chemical bonds

Bond	Bond Energy[a] (kcal/mole)	Wavelength (nm)	Laser	Wavelength range (nm)
-C-H	98	291.7		
-C-C-	83	344.5	Ar^+ (UV)	334-364
Cl-Cl	57.2	499.9	Ar^+ (visible)	458-529
Br-Br	45.2	632.8	He-Ne	632.8
	33.6	850	GaAlAs	800-900
AIBN	31	992		
	26.9	1064	Nd:YAG Nd:Glass	1064
$(C_6H_5)_3-C-C(C_6H_5)_3$	15	1906		

a) AIBN (azobisisobutyronitrile) bond energy from F. M. Lewis and M. S. Matheson, *J. Am. Che Soc.* 71, 747 (1949). All others from S. W. Benson, *J. Chem. Ed.* 42, 503 (1965).

REFERENCES

1. D. Gabor, *Nature* **151**, 777 (1948); *Proc. Roy. Soc.* **A197**, 454 (1949); *Proc. Phys. Soc.* **B54**, 449 (1951).
2. E. N. Leith and J. Upatnieks, *J. Opt. Soc. Am.* **52**, 1123 (1962); *J. Opt. Soc. Am.* **54**, 1295 (1964).
3. R. J. Collier, C. B. Burkhardt and L. H. Lin, *Optical Holography*, Academic Press, New York (1971).
4. H. M. Smith, *Principles of Holography*, Wiley Interscience, New York (1969).
5. H. Kiemle and D. Röss, *Einfurung in die Technik der Holographie*, Akademische Verlagsgesellschaft, Frankfurt am Main (1969).
6. Y. I. Ostrovsky, M. M. Butusov and G. V. Ostrovskaya, "Interferometry by Holography," *Springer Series in Optical Sciences*, Vol. 20, Springer Verlag, Berlin (1980).
7. W. Schuman and M. Dubas, "Holographic Interferometry," *Springer Series in Optical Sciences*, Vol. 16, Springer Verlag, Berlin (1979).
8. G. V. Bally (ed.), "Holography in Medicine and Biology," *Springer Series in Optical Sciences*, Vol. 18, Springer Verlag, Berlin (1979).
9. B. Hill, "Advances in Holography," (N. H. Farhat, ed.), Vol. 3, Marcel Dekker, New York (1977).
10. D. L. Staebler, "Holographic Recording Materials," (H. M. Smith, ed.), *Topics in Appl. Physics* **20**, Springer Verlag, Berlin (1977).
11. D. Casasent, (ed.), "Optical Data Processing," *Topics in Applied Physics*, Vol. 23, Springer Verlag, Berlin (1978).
12. S. H. Lee, (ed.), "Optical Information Processing," *Topics in Applied Physics*, Vol. 48, Springer Verlag, Berlin (1981).

13. B. J. Chang and C. D. Leonard, *Appl. Optics* **18**, 2407 (1979).

14. D. H. CLose, *Opt. Eng.* **14**, 408 (1975).

15. V. E. Wood, N. F. Hartman, C. M. Verber and R. P. Kenan, *J. Appl. Phys.* **46**, 1214 (1975); W. J. Tomlinson, H. P. Webber, C. A. Pryde and E. A. Chandross, *Appl. Phys. L* **26**, 303 (1975); T. Tamir, (ed.), "Integrated Optics," *Topics in Applied Physics*, Vol. 7, Springer Verlag, Berlin (1979); A. Wuthrich and W. Lukosz, *Appl. Phys.* **21**, 55 (1980).

16. W. S. Boyle, *Spektrum d. Wissenschaft, Erstedition*, **1**, 72 (1979).

17. A. L. Schawlow and C. H. Townes, *Phys. Rev.* **112**, 1940 (1958).

18. E. Garmire, "Integral Optics," (T. Tamir, ed.), *Topics in Applied Physics*, Vol. 7, Springer Verlag, Berlin (1979).

19. H. Kogelnik, *Bell System Tech. J.* **48**, 2909 (1969).

20. D. M. Burland and Chr. Bräuchle, *J. Chem. Phys.* **76**, 4502 (1982).

21. J. D. Jackson, *Classical Electrodynamics*, Wiley, New York (1962), p. 155.

22. Z. G. Szabo, *Theory of Kinetics,* (C. H. Bamford and C. F. H. Tipper, eds.), Elsevier, Amsterdam (1969).

23. G. C. Bjorklund, D. M. Burland and D. C. Alvarez, *J. Chem. Phys.* **73**, 4321 (1980).

24. D. M. Burland, G. C. Bjorklund and D. C. Alvarez, *J. Am. Chem. Soc.* **102**, 7117 (1980).

25. F. W. Deeg, J. Pinsl, Chr. Bräuchle and J. Voitländer, to be published.

26. Chr. Bräuchle, *Mol. Cryst. Liq. Cryst.* in press.

27. M. V. George and J. C. Scaiano, *J. Phys. Chem.* **84**, 492 (1980).

28. J. N. Pitts, Jr., J. K. S. Wan and E. A. Schuck, *J. Am. Chem. Soc.* **86**, 3006 (1964).

29. Chr. Bräuchle, D. M. Burland and G. C. Bjorklund, *J. Phys. Chem.* **85**, 123 (1981) and **85**, 618 (1981) correction.

30. G. O. Schenk, M. Cziesla, K. Eppinger, G. Matthias and M. Pape, *Tetrahedron Lett.* **193**, (1967); G. O. Schenk and G. Matthias, *Tetrahedron Lett.* 193 (1967).

31. N. Filipescu and F. L. Minn, *J. Am. Chem. Soc.* **90**, 1544 (1968).

32. J. Chilton, L. Giering and C. Steel, *J. Am. Chem. Soc.* **98**, 1865 (1976).

33. H. Murai and K. Obi, *J. Phys. Chem.* **79**, 2446 (1975); M. Murai, M. Jinguji and K. Obi *J. Phys. Chem.* **82**, 38 (1978).

34. Chr. Bräuchle, D. M. Burland and G. C. Bjorklund, *J. Am. Chem. Soc.* **103**, 2515 (1981).

35. D. M. Burland, *Proc. SPIE* **113**, 151 (1977); D. M Burland, F. Carmona and J. Pacansky, *Chem. Phys. Lett.* **56**, 221 (1978).

36. B. Dellinger, M. A. Paczkowski, R. M. Hochstrasser and A. B. Smith III, *J. Am. Chem. Soc.* **100**, 3242 (1978).

37. D. M. Burland and F. Carmona, *Mol. Cryst. Liq. Cryst.* **50**, 279 (1979).

38. H. de Vries and D. A. Wiersma, *J. Chem. Phys.* **72**, 1851 (1980).

39. M. Paczkowski, R. Pierce, A. B. Smith III and R. M. Hochstrasser, *Chem. Phys. Lett.* **72**, 5 (1980).

40. (a) U. Schmitt and D. M. Burland, *J. Chem. Phys.*, in press. (b) Chr. Bräuchle, *Nachr. Chem. Techn. Lab.* **29**, 603 (1981).

41. N. J. Turro, V. Ramamurthy, W. Cherry and W. Farneth, *Chem. Rev.* **78**, 125 (1978).

42. R. Loudon, *The Quantum Theory of Light*, Clarendon Press, Oxford (1973), p. 56 ff.

43. P. Crabbé, *ORD and CD in Chemistry and Biochemistry*, Academic Press, New York (1972). H. B. Kagan (ed.), *Stereochemistry*, Vol. 2, Thieme Verlag, Stuttgart (1977).

44. S. L. Shapiro (ed.), "Ultrashort Light Pulses," *Topics in Applied Physics* **18**, Springer Verlag, Berlin (1977).

45. D. W. Phillion, D. J. Kuizenga and E. A. Siegman, *Appl. Phys. Lett.* **27**, 85 (1975) and references therein.

46. H. J. Eichler, *Optica Acta* **24**, 631 (1977) and references therein.

47. M. D. Fayer, *Ann. Rev. Phys. Chem.* **33**, 63 (1982).

48. H. Boersch and H. J. Eichler, *Z. Angew. Phys.* **22**, 378 (1967).

49. H. J. Eichler, G. Salje and H. Stahl, *J. Appl. Phys.* **44**, 5383 (1973).

50. H. J. Eichler, P. Glotzbach and B. Kluzowski, *Z. Angew. Phys.* **28**, 303 (1970).

51. R. S. Moog, M. D. Ediger, S. G. Boxer and M. D. Fayer, *J. Phys. Chem.* **86**, 4694 (1982).

52. F. W. Deeg, J. Pinsl and Chr. Bräuchle, unpublished results.

53. J. R. Salcedo, A. E. Siegmann, D. D. Dlott and M. D. Fayer, *Phys. Rev. Lett.* **41**, 131 (1978).

54. D. R. Lutz, R. A. Nelson, C. R. Gochanour and M. D. Fayer, *Chem. Phys.* **58**, 325 (1981).

55. R. Baltramiejunas, K. Jarasinomas, J. Vaikus and D. Veleckas, *Opt. Commun.* **18**, 47 (1976).

56. D. M. Friedrich and S. A. Klem, *Chem. Phys.* **41**, 153 (1979).

57. Chr. Bräuchle, Habilitationsschrift, Universität München, (1982).

58. A. S. Davydov, *Theory of Molecular Excitons*, Plenum Press, New York (1971).

59. I. Beriman, *Energy Transport Properties of Aromatic Compounds*, Academic Press, New York (1973).

60. D. M. Burland and A. H. Zewail, *Adv. Chem. Phys.* **40**, 369 (1979).

61. T. Markvart, *J. Theor. Biol.* **72**, 91 (1978).

62. J. R. Norris, M. E. Druyan and J. J. Katz, *J. Am. Chem. Soc.* **95**, 1680 (1973). F. K. Fong, *Appl. Phys.* **6**, 151 (1975); M. C. Thurnaver, J. J. Katz and J. R. Norris, *Proc. Nat. Acad. Sci. USA* **72**, 3270 (1975).

63. H. G. Danielmeyer, *J. Appl. Phys.* **42**, 3125 (1971).

64. D. R. Dean and J. R. Collins, *J. Appl. Phys.* **44**, 5455 (1973).

65. R. Orlowski, *Phys. Blatter* **37**, 365 (1981).

66. R. Orlowski and E. Krätzig, *Solid State Commun.* **27**, 1351 (1978); *Ferroelectrics* **26**, 831 (1980); *Ferroelectrics* **27**, 241 (1980).

67. K. H. Richter, W. Güttler and M. Schwoerer, *Chem. Phys. Lett.* (1982).

68. G. R. Fleming, J. M. Morris and G. W. Robinson, *Chem. Phys.* **17**, 91 (1976).

69. S. A. Rice and G. A. Kenney-Wallace, *Chem. Phys.* **47**, 161 (1980).

70. A. von Jena and H. E. Lessing, *Opt. Quant. Elect.* **11**, 419 (1979).

71. Chr. Bräuchle, unpublished results.

72. G. R. Fleming, A. E. Knight, J. M. Morris, R. J. Robbins and G. W. Robinson, *Chem. Phys. Lett.* **49**, 1 (1977).

73. A. von Jena and H. E. Lessing, *Chem. Phys.* **40**, 245 (1979); *Chem. Phys. Lett.* **78**, 187 (1981).

74. G. S. Beddard, T. Doust and J. Hudales, *Nature* **294**, 145 (1981).

75. A. Einstein, *Ann. Physik* **19**, 371 (1906).

76. K. B. Eisenthal and K. H. Drexhage, *J. Chem. Phys.* **51**, 5720 (1969).

77. G. R. Gochanour, H. C. Anderson and M. D. Fayer, *J. Chem. Phys.* **70**, 4254 (1979) and references therein.

78. J. E. Selwyn and J. I. Steinfeld, *J. Phys. Chem.* **76**, 762 (1972).

79. J. B. Birks, *Photophysics of Aromatic Molecules* Wiley, New York (1970).

80. K. A. Nelson and M. D. Fayer, *J. Chem. Phys.* **72**, 5202 (1980).

81. J. R. Andrews and R. M. Hochstrasser, *Chem. Phys. Lett.* **76**, 213 (1980).

82. K. A. Nelson, R. Casalegno, R. J. D. Miller and M. D. Fayer, *J. Chem. Phys.* **77**, 1144 (1982).

83. D. Pohl, M. Maier and W. Kaiser, *Phys. Rev. Lett.* **20**, 366 (1968).

84. K. A. Nelson, D. R. Lutz and M. D. Fayer, *Phys. Rev. B*, **24**, 3261 (1981).

85. M. R. B. Forshaw, *Opt. and Laser Tech.*, February (1974), p. 28; R. L. Kurtz and R. B. Owen, *Opt. Eng.* **14**, 393 (1974); P. Hariharan, *ibid.* **19**, 636 (1980).

86. W. J. Tomlinson and E. A. Chandross, *Adv. Photochem.* **12**, 201 (1980).

87. B. J. Chang, *Opt. Eng.* **19**, 642 (1980).

88. K. Tatsuno and A. Arimoto, *Appl. Opt.* **19**, 2096 (1980).

89. G. C. Bjorklund, Chr. Bräuchle, D. M. Burland and D. C. Alvarez, *Opt. Lett.* **6**, 159 (1981).

90. Chr. Bräuchle, U. P. Wild, D. M. Burland, G. C. Bjorklund and D. C. Alvarez, *Opt. Lett.* **7**, 177 (1982); *IBM J. of Res. and Dev.* **26**, 217 (1982).

91. D. von der Linde, A. M. Glass and K. F. Rodgers, *Appl. Phys. L* **25**, 155 (1974).

92. D. von der Linde, A. M. Glass and K. F. Rodgers, *Appl. Phys. L* **26**, 22 (1974).

93. D. von der Linde, A. M. Glass and K. F. Rodgers, *J. Appl. Phys.* **47**, 217 (1976).

94. V. Gerbig, R. K. Grygier, D. M. Burland and G. Sincerbox, to be published.

95. D. H. Close, *Opt. Eng.* **14**, 408 (1975); B. J. Chang and C. D. Leonard, *Appl. Opt.* **18**, 2407 (1979); Yu. S. Mosyakin and G. V. Skrotski, *Sov. J. Quant. Electron* **2**, 199 (1972); C. S. Ih, *Appl. Opt.* **17**, 748 (1978); R. V. Pole, H. W. Werlich and R. J. Krusche, *Appl. Opt.* **17**, 3249 (1978); S. K. Case and V. Gerbig, *Opt. Eng.* **19**, 711 (1980).

96. P. K. Tien, *Appl. Opt.* **10**, 2395 (1971); W. S. C. Chang, *IEEE Trans. Microwave Th. and Tech. MTT21*, 755 (1973).

97. V. Gerbig, R. K. Grygier, D. M. Burland and G. Sincerbox, unpublished results.

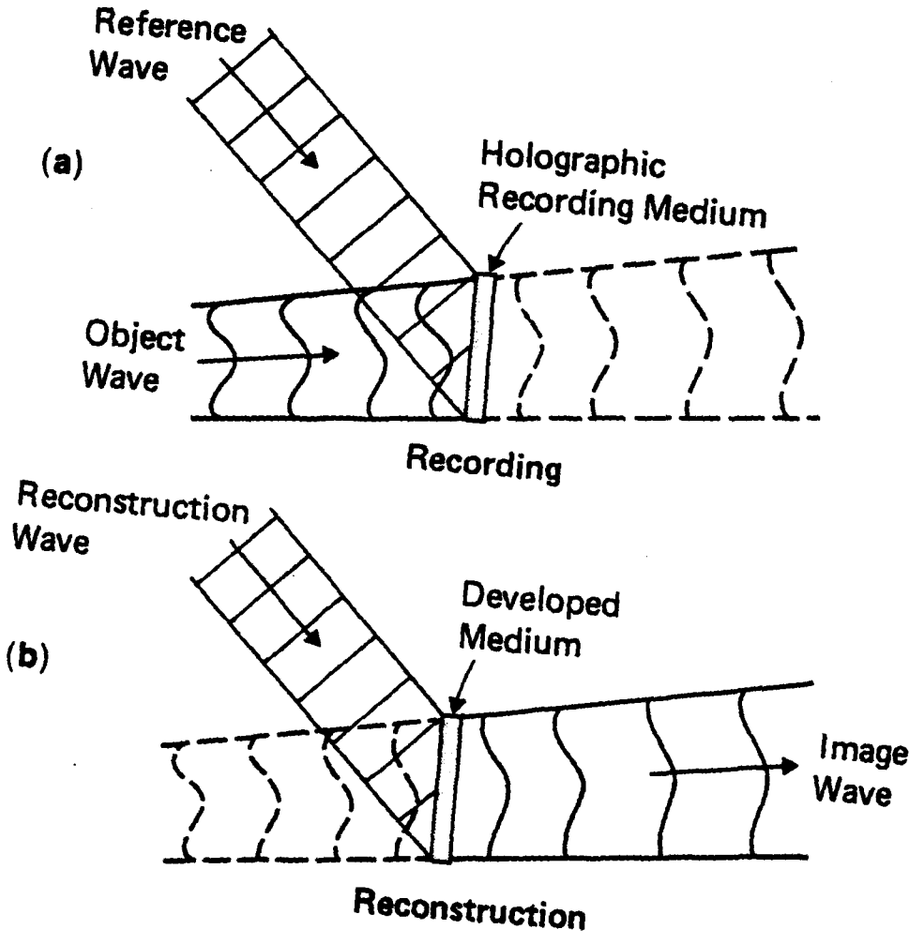

Figure 1. Schematic representation of the holographic recording (a) and reconstruction (b) procedures.

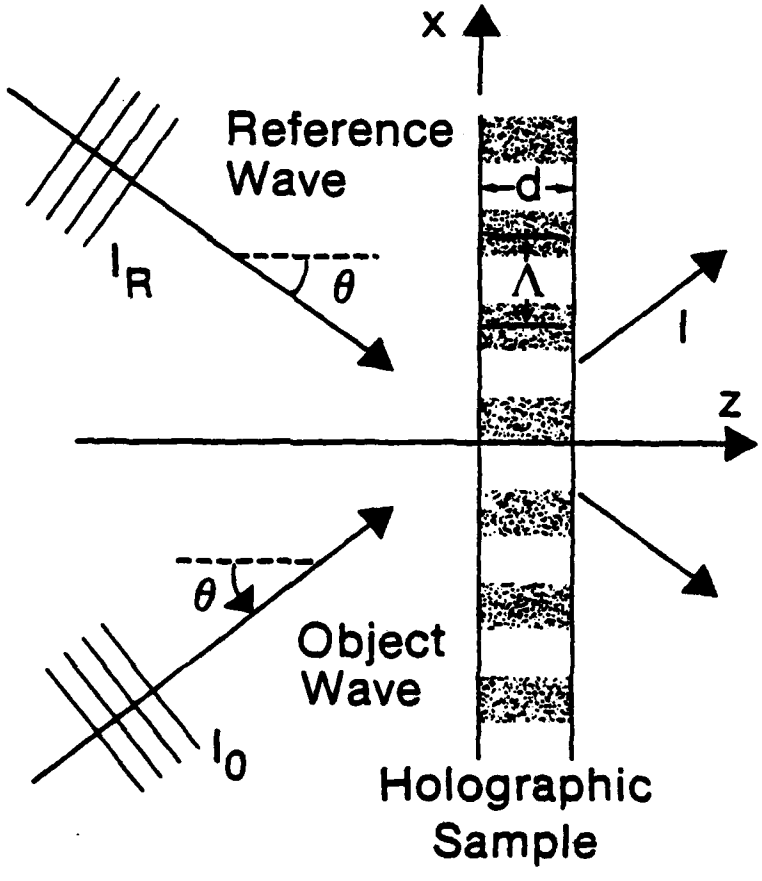

Figure 2. The production of a plane wave hologram.

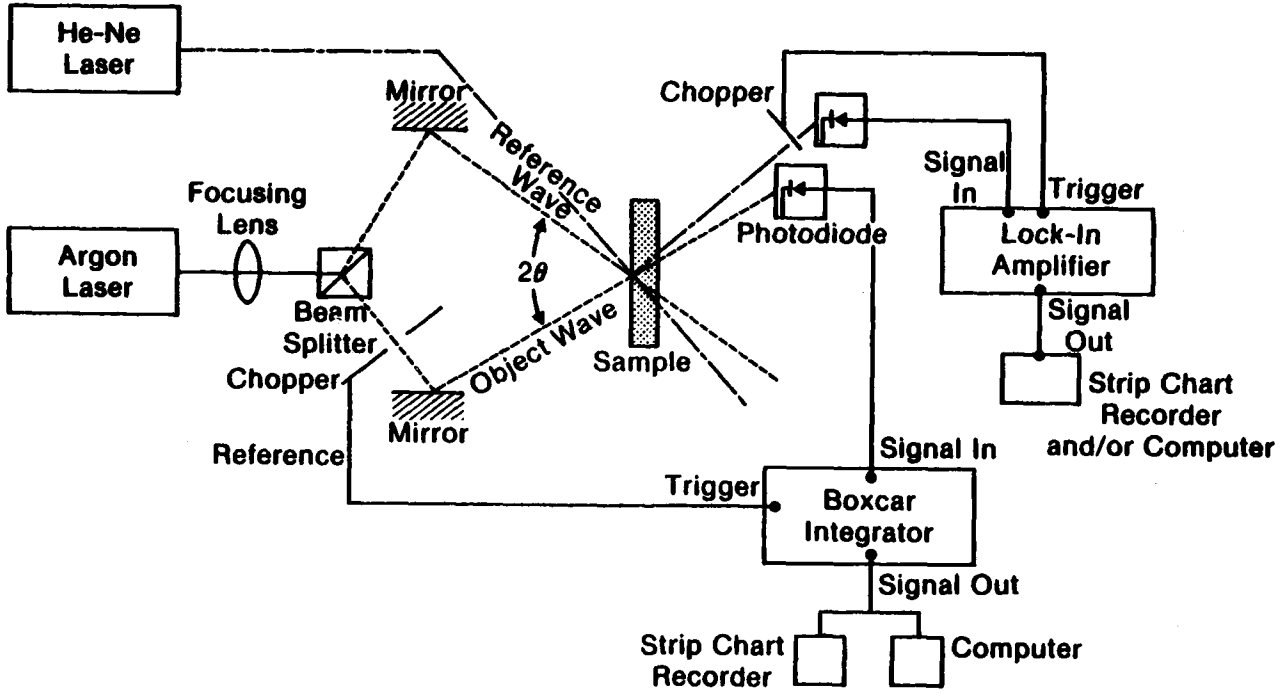

Figure 3. A schematic representation of the apparatus for the detection of holographic growth curves. The detection method using a third He-Ne laser is indicated by the dash-dotted line. The method using a chopper in the object beam is shown by the dashed line.

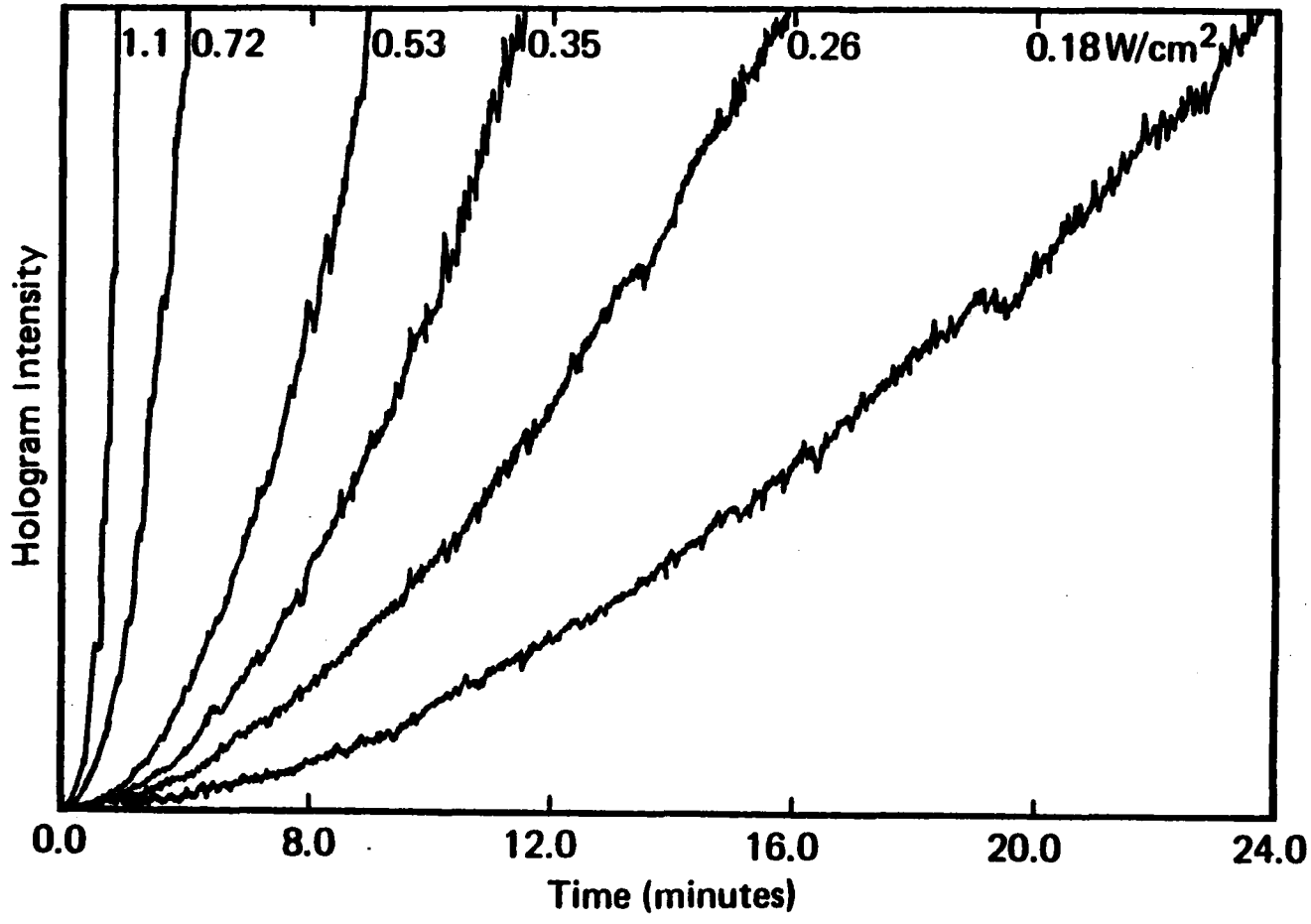

Figure 4. Hologram growth curves for different intensities of the hologram forming beams. Only the early stages of the hologram growth are shown. These results were obtained with a dimethyl-s-tetrazine sample in polyvinylcarbazole using the 514.5 nm line from an argon ion laser.

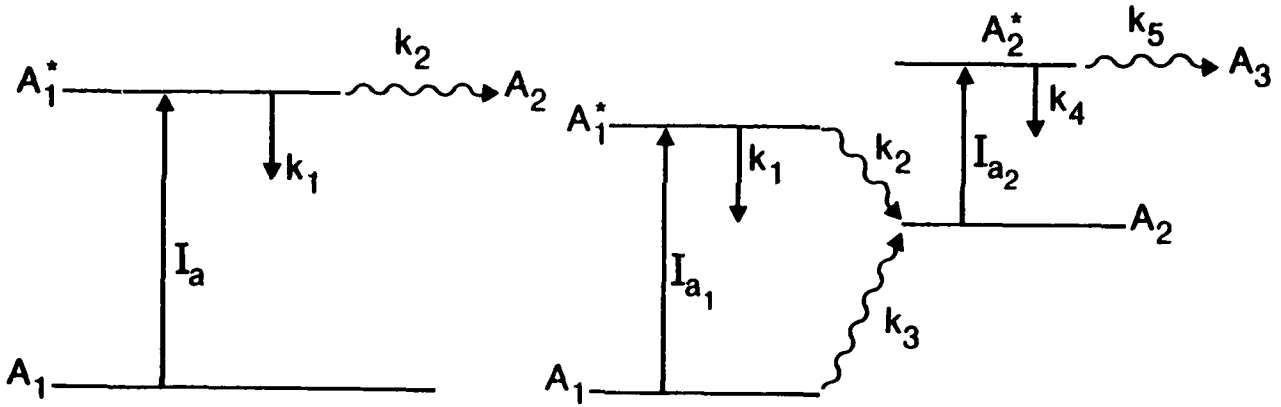

$$\Phi_P = \frac{k_2}{k_1 + k_2}$$

$$\Phi_P = \frac{k_5}{k_4 + k_5}\ ,\quad \Phi = \frac{k_2}{k_1 + k_2}$$

Figure 5. Level schemes for a one-photon two-level (left side) and a two-photon four-level (right side) photoreaction. The rate constants and the quantum yields for the kinetic processes are indicated as are expressions for the quantum yields.

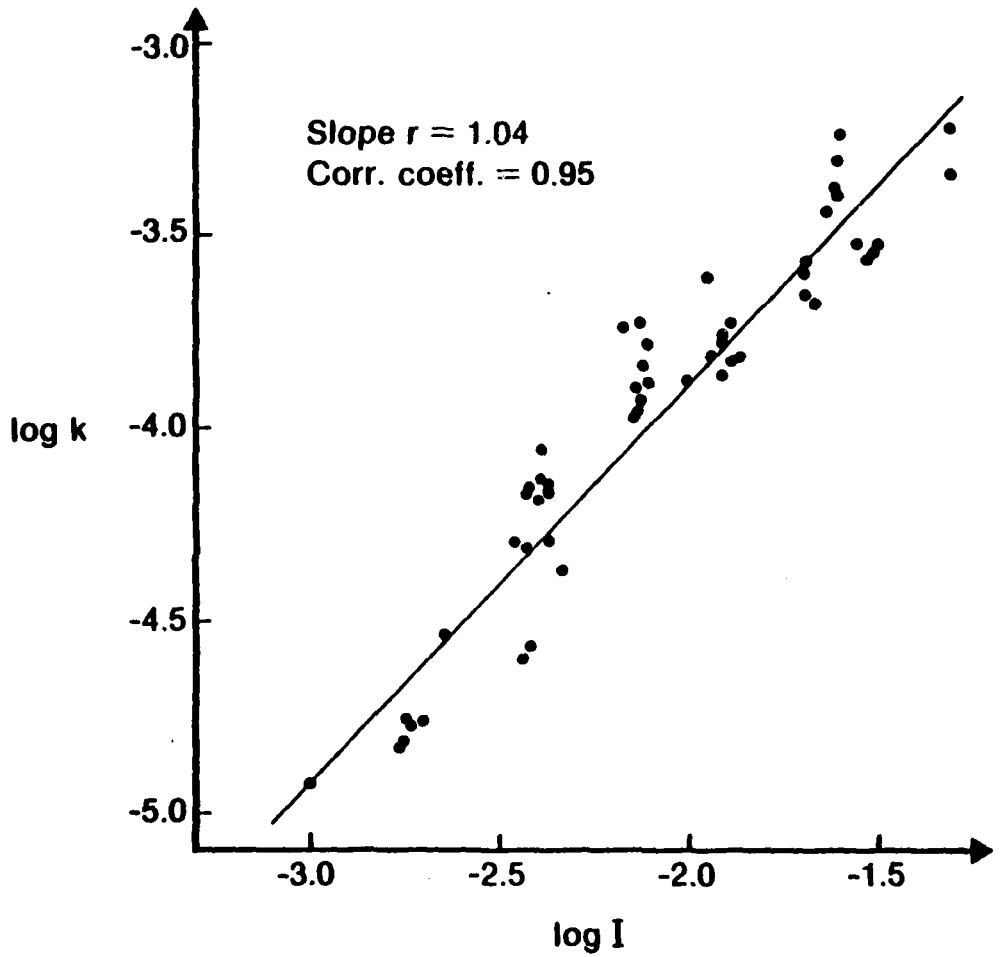

Figure 6. A double logarithmic plot of the overall rate constant k as a function of intensity I for the holographically observed photoreaction of o-nitrobenzaldehyde.

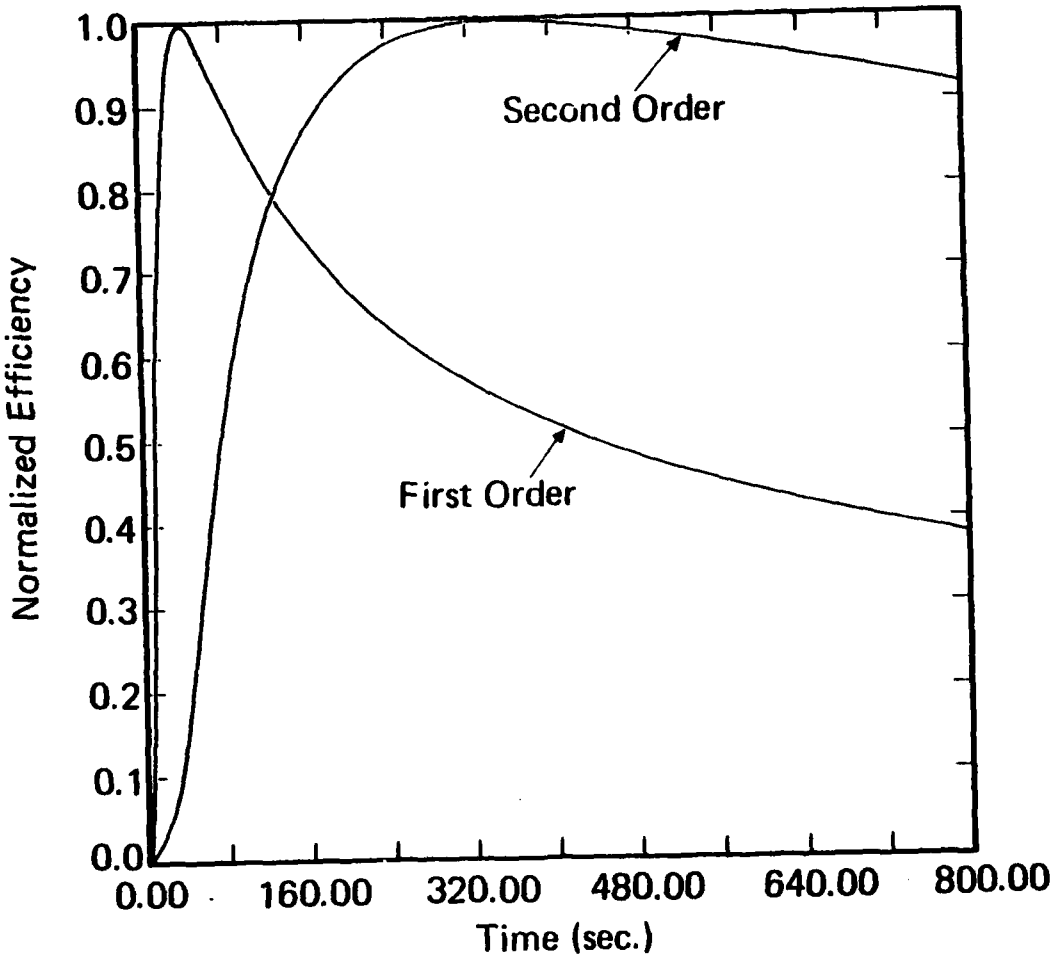

Figure 7. Calculated hologram growth curves for first and second order holograms. Both curves have been normalized to maximum efficiencies of unity.

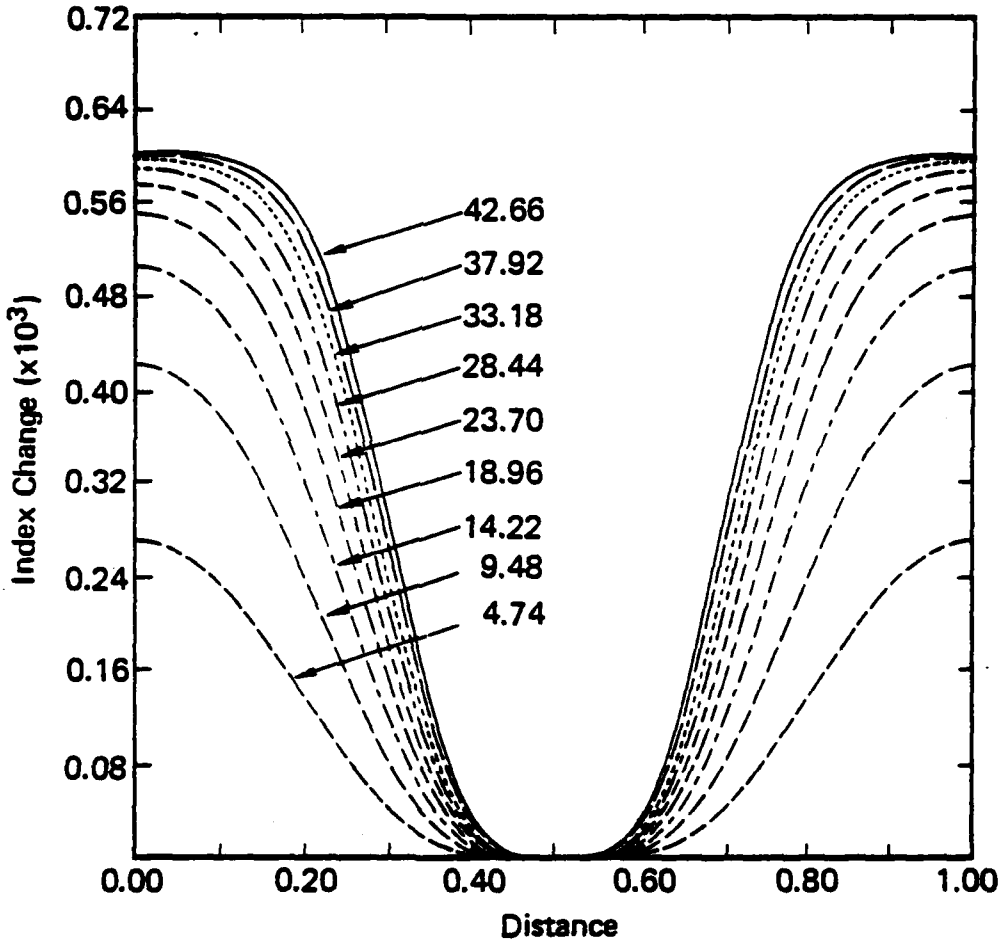

Figure 8. The index of refraction change across one period Λ of the holographic grating for a one-step photoreaction for various illuminations. (The distance is in units of Λ.)

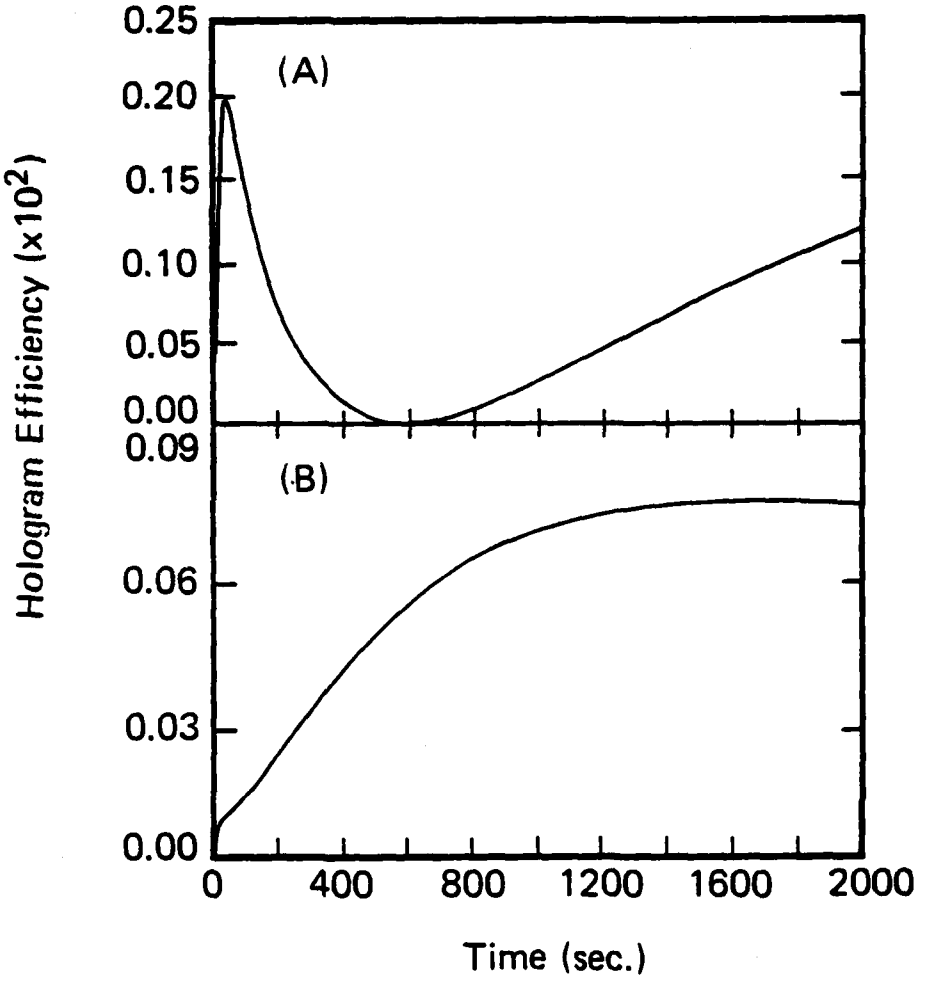

Figure 9. Calculated hologram efficiency *versus* time for a consecutive reaction scheme $A_1 \rightarrow A_2 \rightarrow A_3$. (a) Additive and (b) subtractive behavior of the change of the index of refraction in the two reaction steps.

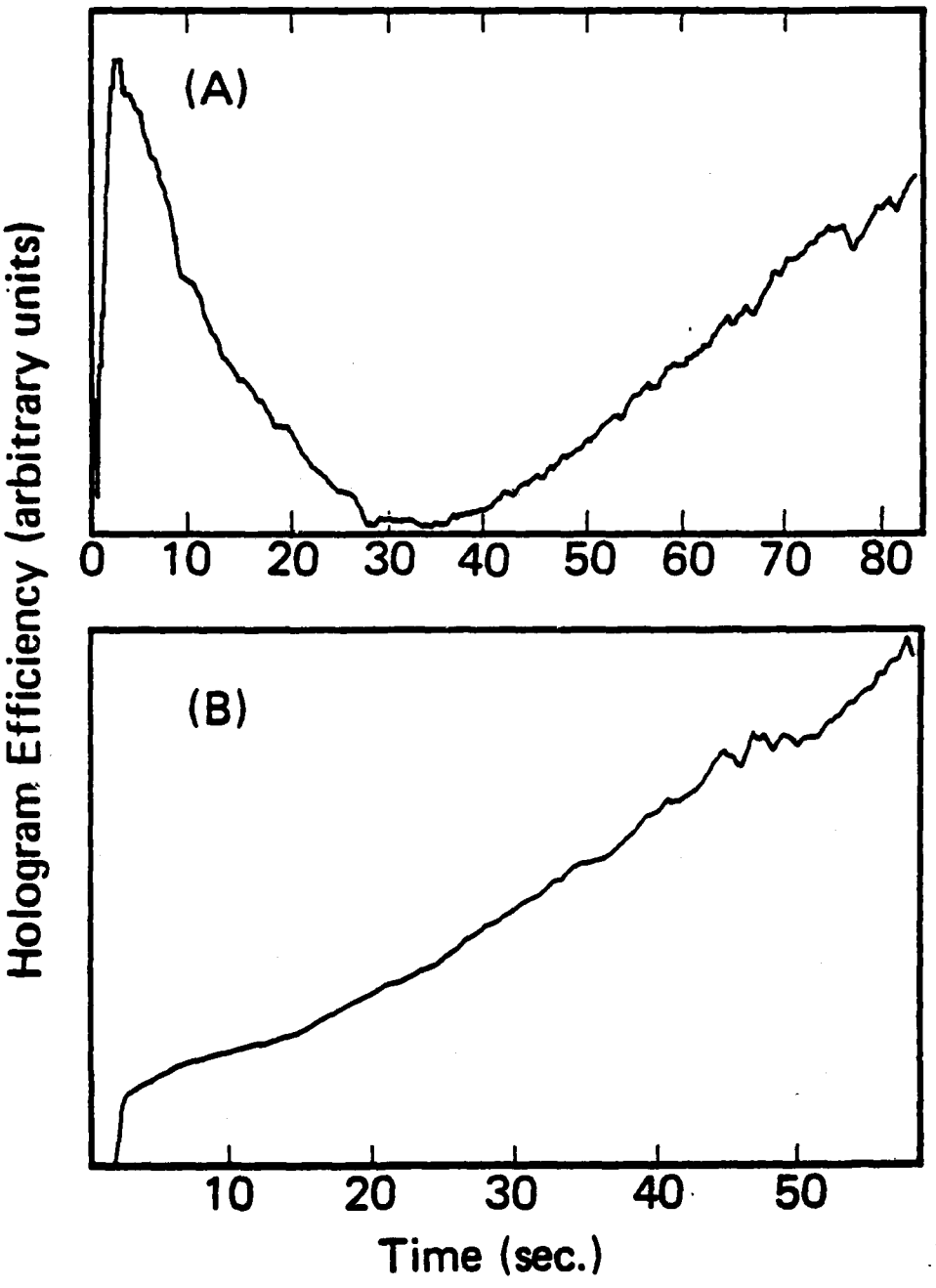

Figure 10. Experimental hologram efficiency *versus* time for a 250 μm thick sample of 5% by weight benzophenone in PMMA. The hologram was produced using the UV-lines of an Ar^+ laser and read with (a) the 514 nm line and (b) with the UV lines of an Ar^+ laser.

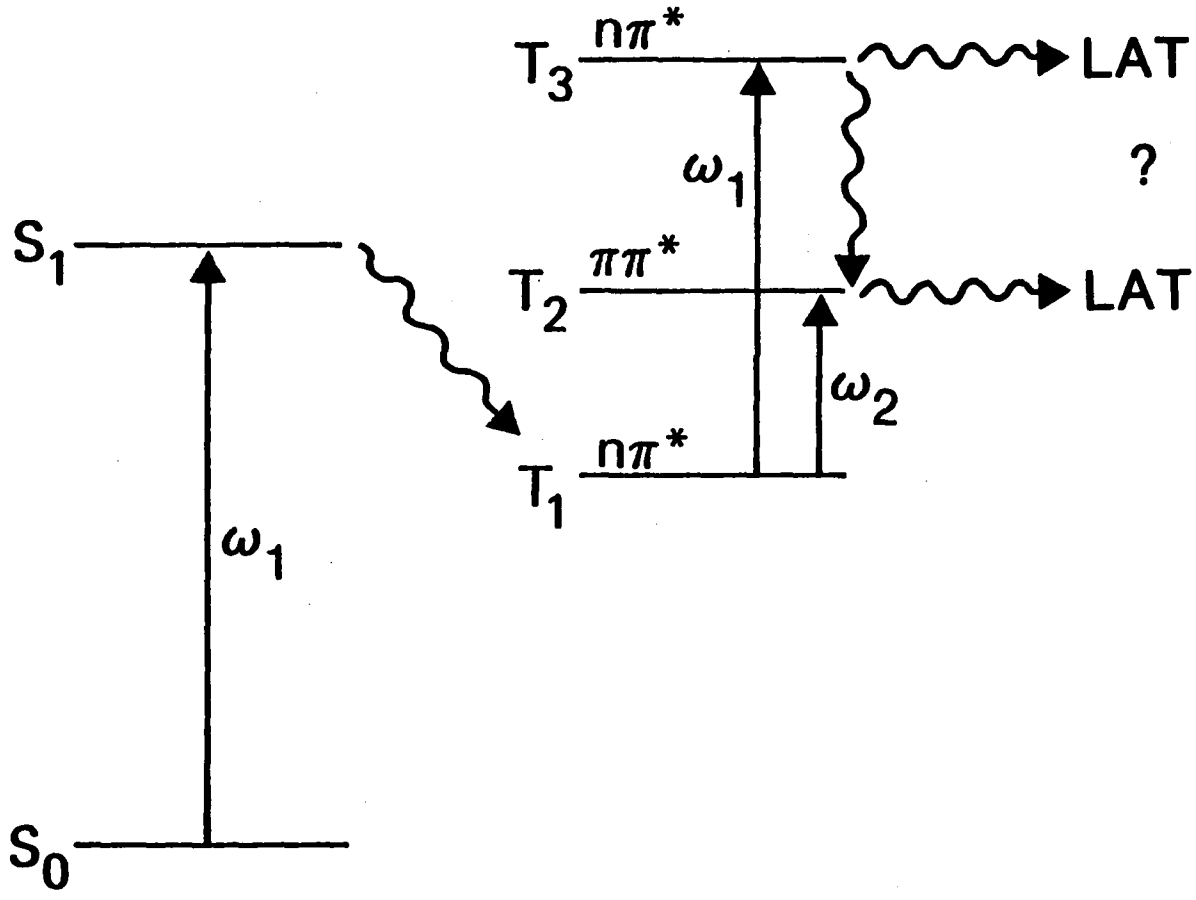

Figure 11. The level scheme for the first step of the photoreaction of benzophenone to the light absorbing transient (LAT) involving the absorption of two photons. Two possible pathways to the LAT are suggested.

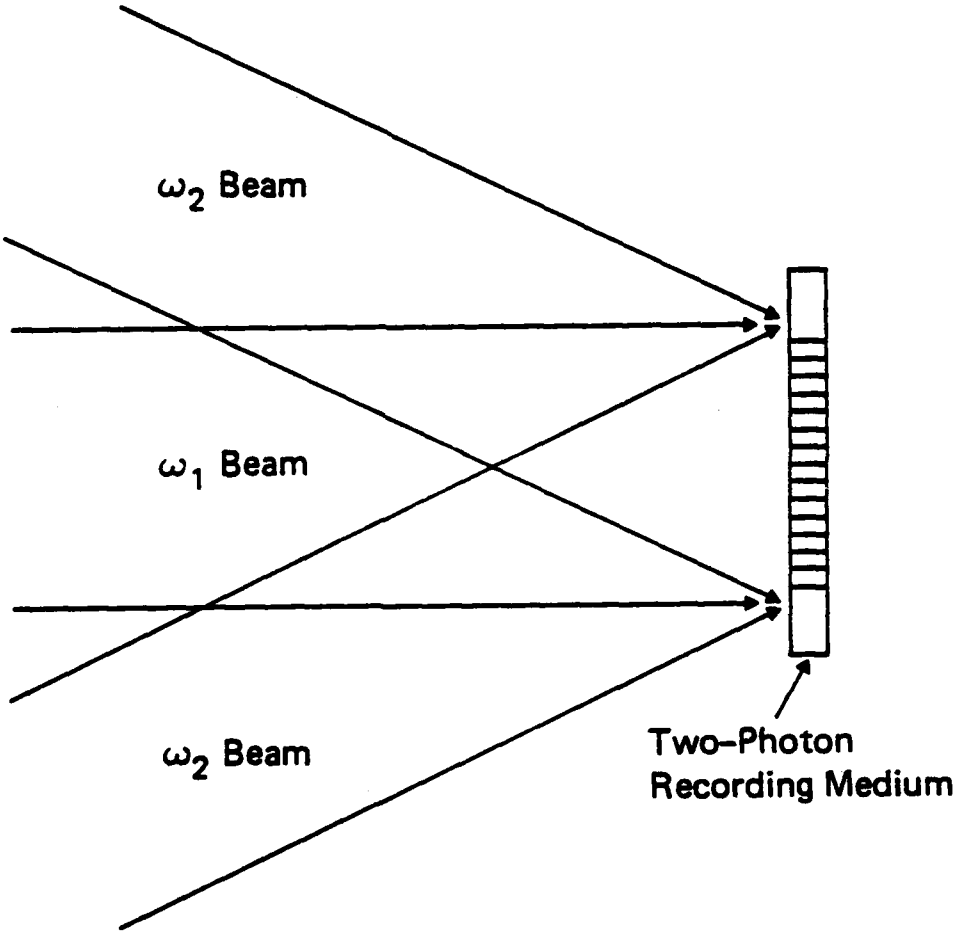

Figure 12. A three-beam experiment using two different light sources. Only the beam at ω_2 needs to be coherent and only these beams can produce a hologram.

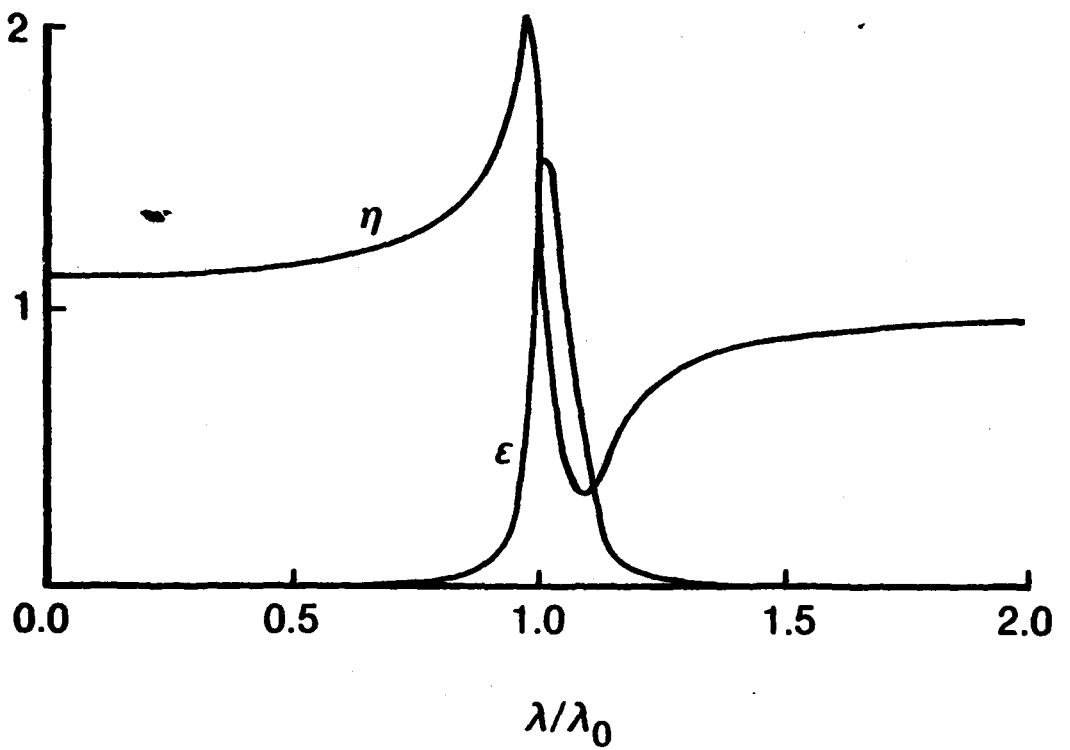

Figure 13. The dispersion curve n *versus* λ and the absorption curve *e versus* λ for an optical transition at wavelength λ_0. The abscissa is in units of λ/λ_0.

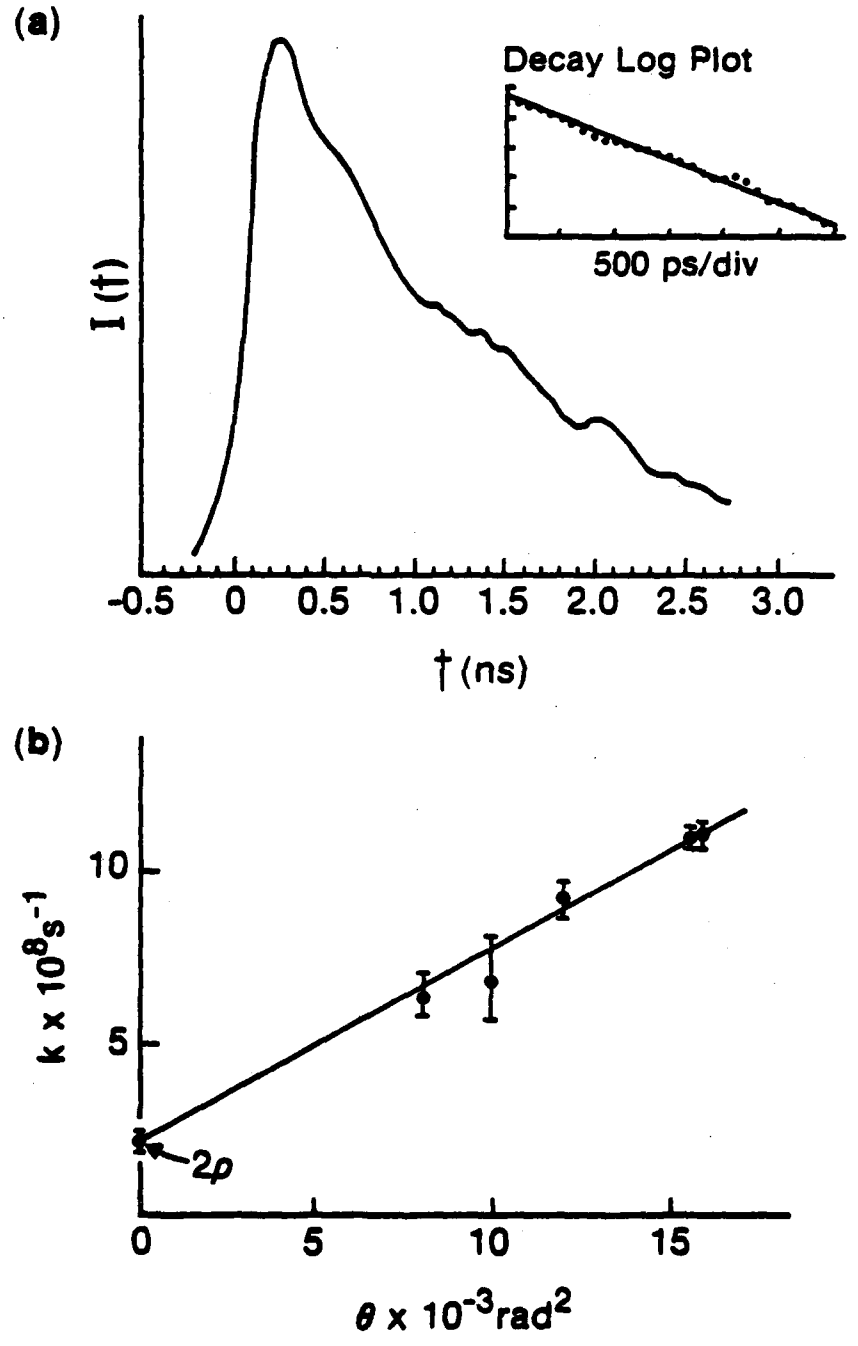

Figure 14. (a) The decay of the diffracted probe pulse intensity *versus* probe pulse delay time. The inlay shows the logarithmic plot giving the decay rate k as the slope. (b) The transient grating decay rate k *versus* the square of the angle of incidence θ^2 giving the diffusion constant D as the slope and $2/\tau$ as the intercept. Figure 14(a) and (b) are obtained from Ref. 53.

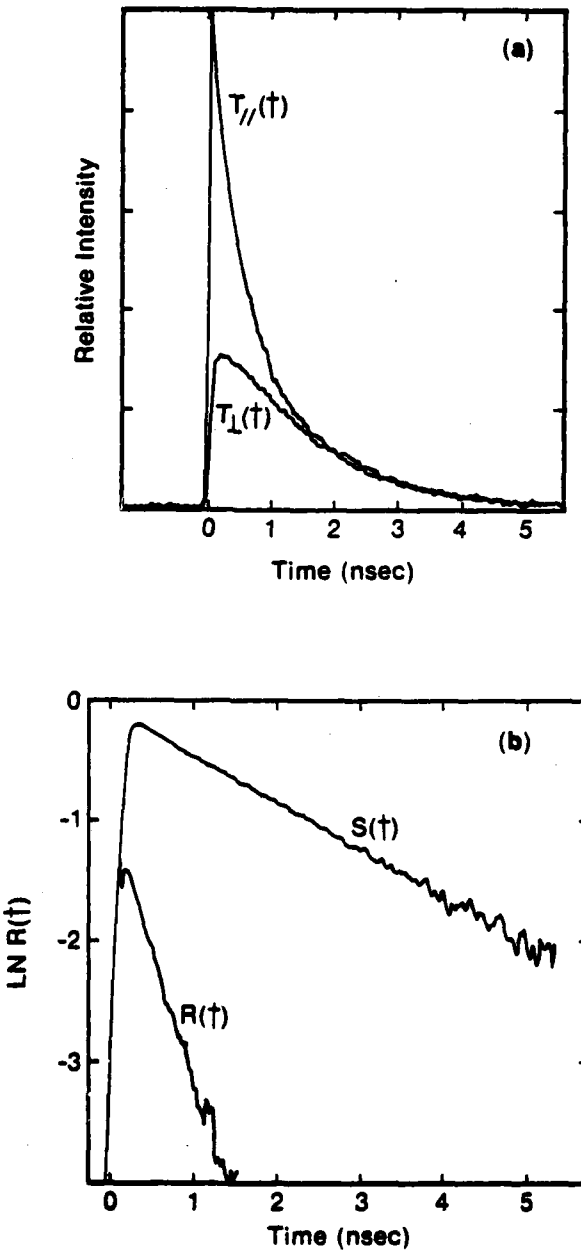

Figure 15. (a) The decay of the transient grating signal with probe pulse polarization parallel to ($I_{//}(t)$) and perpendicular to ($I_{\perp}(t)$) the excitation polarization for a sample of Rhodamine B in n-propanol. (b) S(t) and R(t) curves calculated from the data presented in (a). The straight lines fits yield values of the excited state lifetime τ and the orientational reorientation time τ_R.

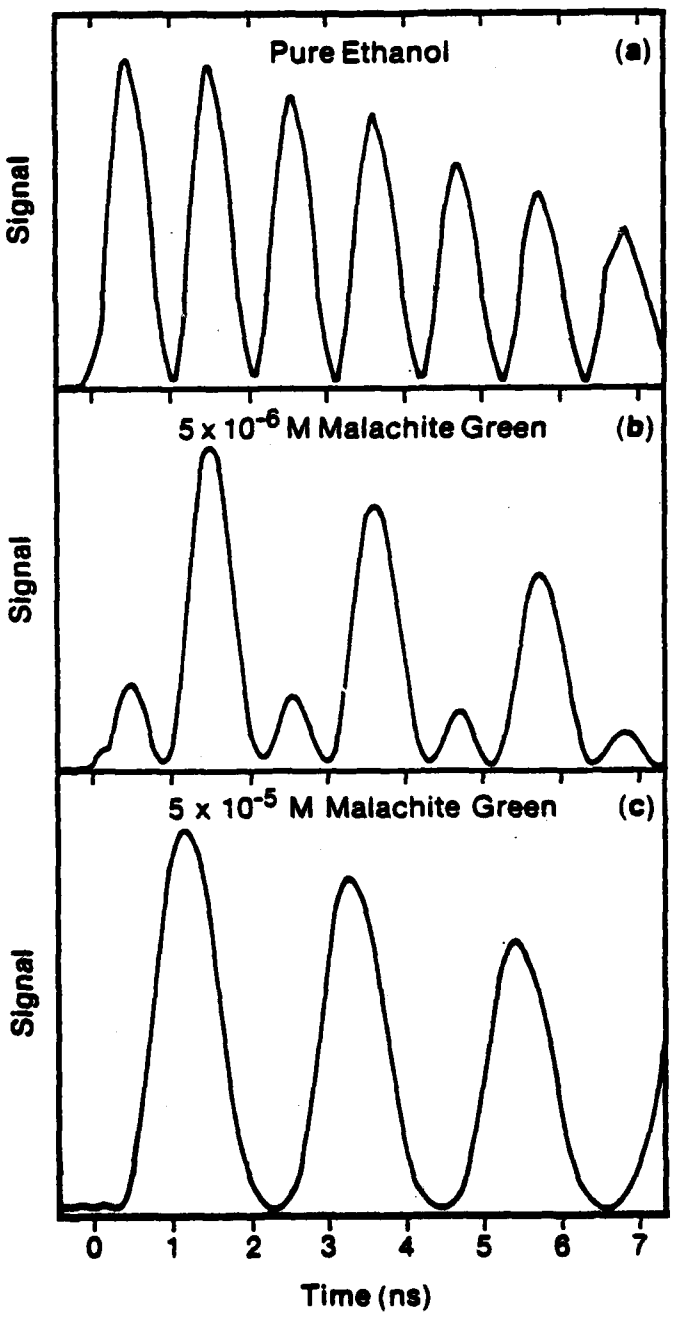

Figure 16. Optically generated ultrasonic waves detected in (a) pure ethanol and increasing concentrations (b) → (c) of malachite green in ethanol. In pure ethanol (a), the Brillouin scattering is responsible whereas in concentrated solutions of malachite green (c), the heating effect due to absorption accounts for the generation of ultrasonic waves; (b) represents an intermediate case. Figure 16(a), (b) and (c) are obtained from Ref. 47.

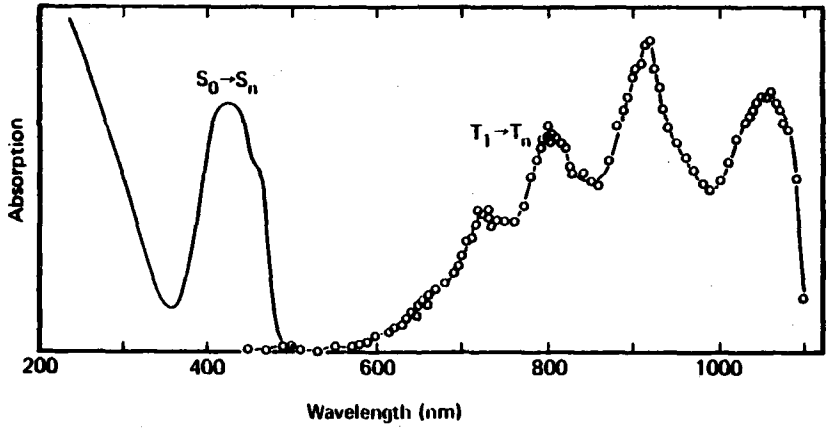

Figure 17. The $S_0 \rightarrow S_n$ and $T_1 \rightarrow T_n$ absorption spectra for biacetyl. The $S_0 \rightarrow S_n$ absorption is for a 15% concentration of biacetyl in a 300 μm thick sample of cyanoacrylate and the $T_1 \rightarrow T_n$ absorption is for a 3.9×10^{-2}M solution of biacetyl in carbon tetrachloride.

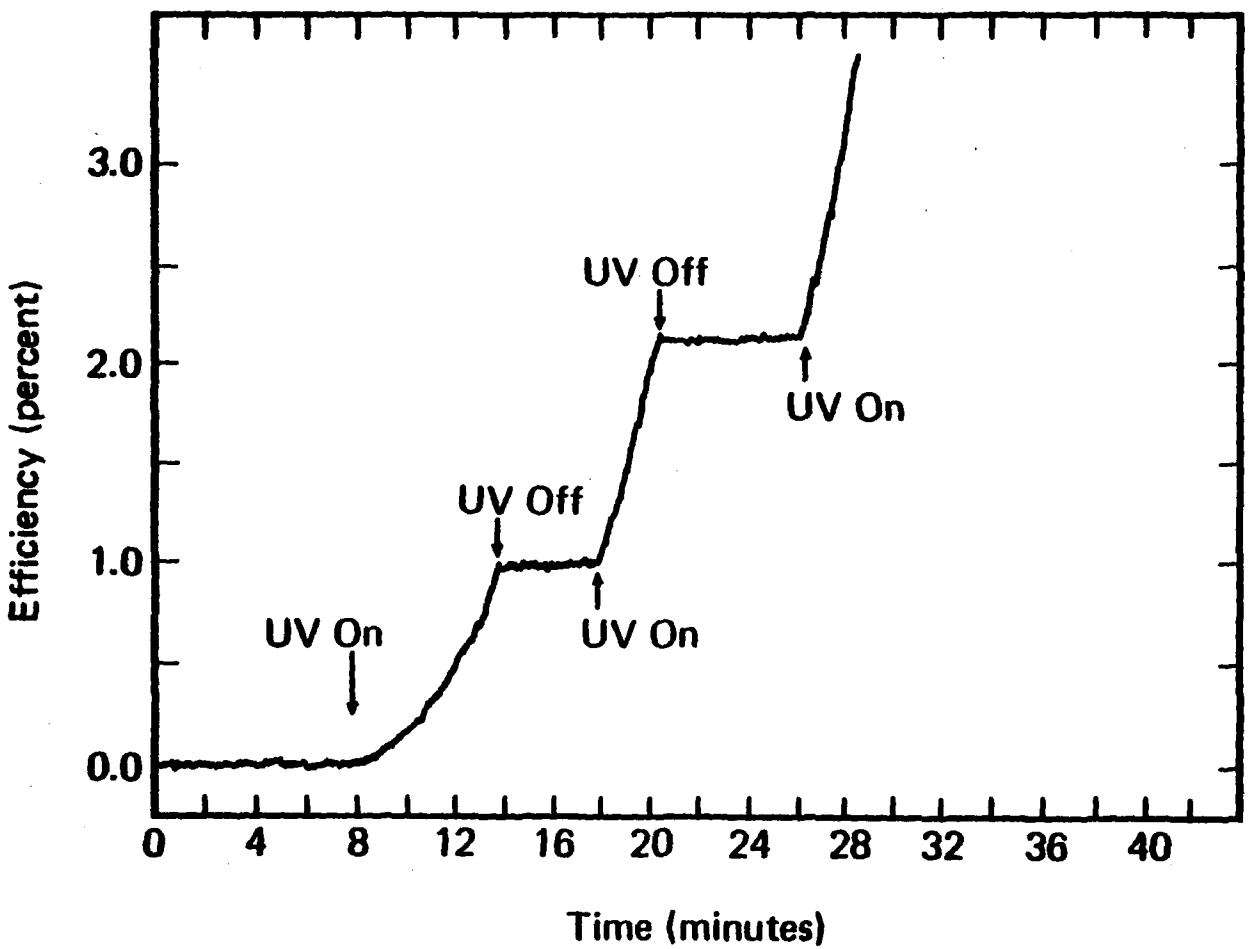

Figure 18. Gating of a hologram in a 15% biacetyl in polycynaoacrylate sample.

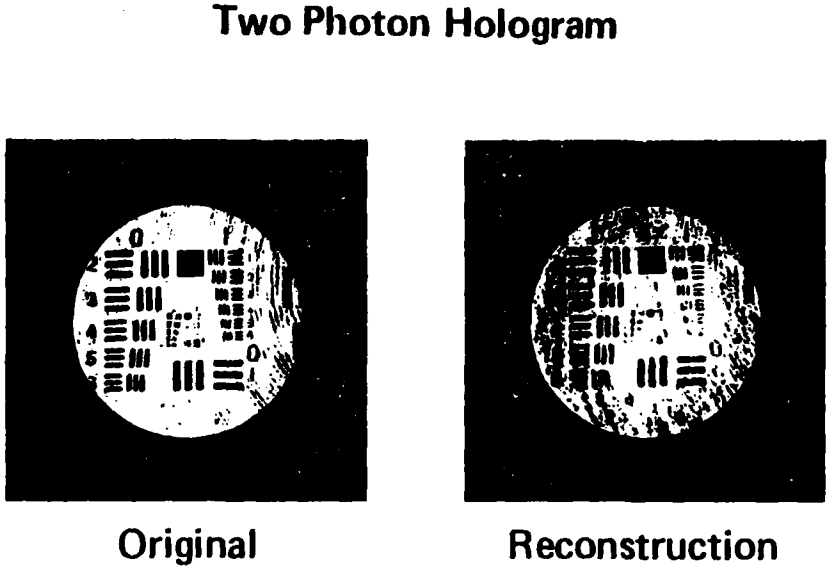

Figure 19. Two-photon hologram of a resolution chart.

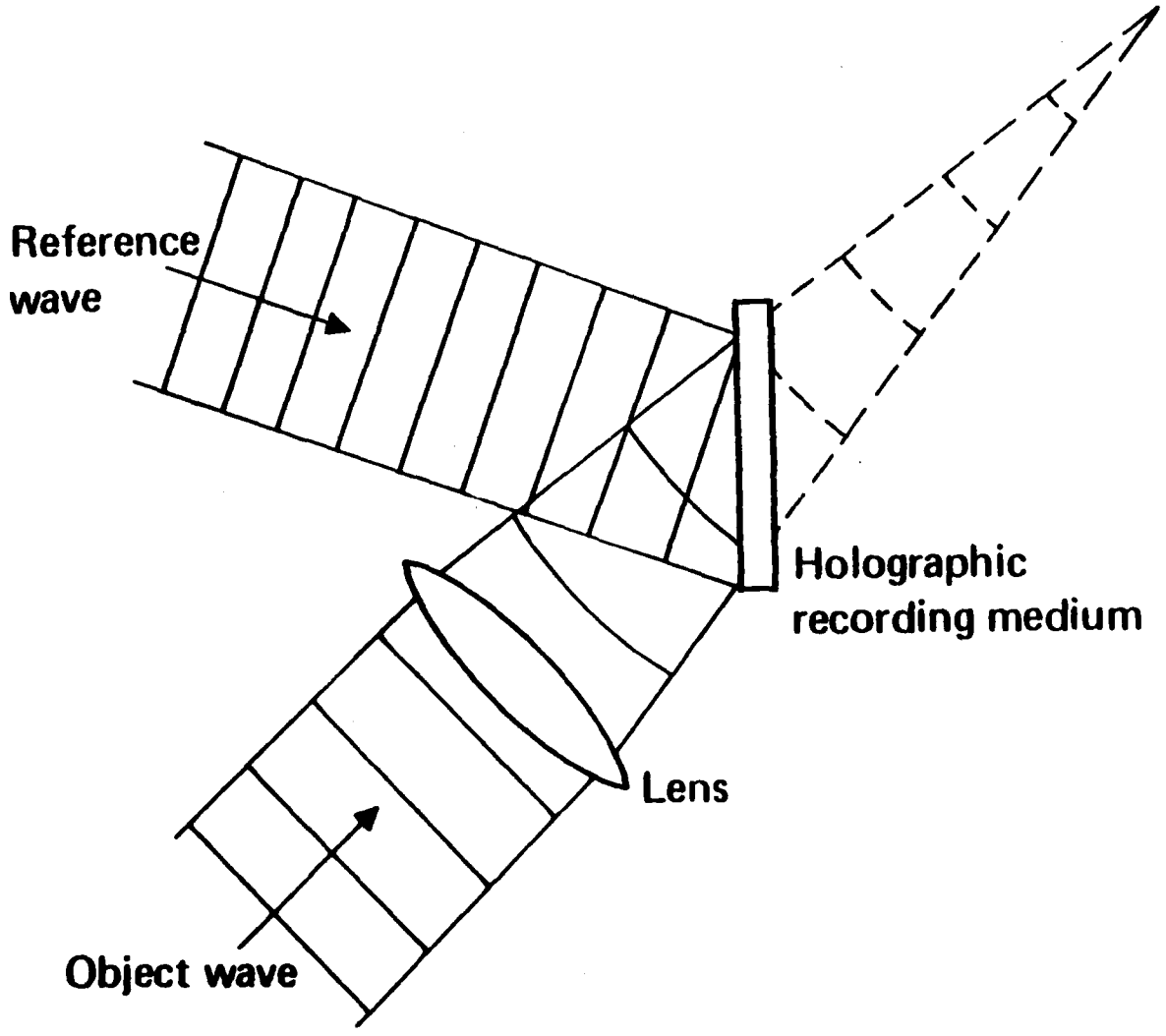

Figure 20. The arrangement of the coherent light waves necessary to record the holographic image of a lens.

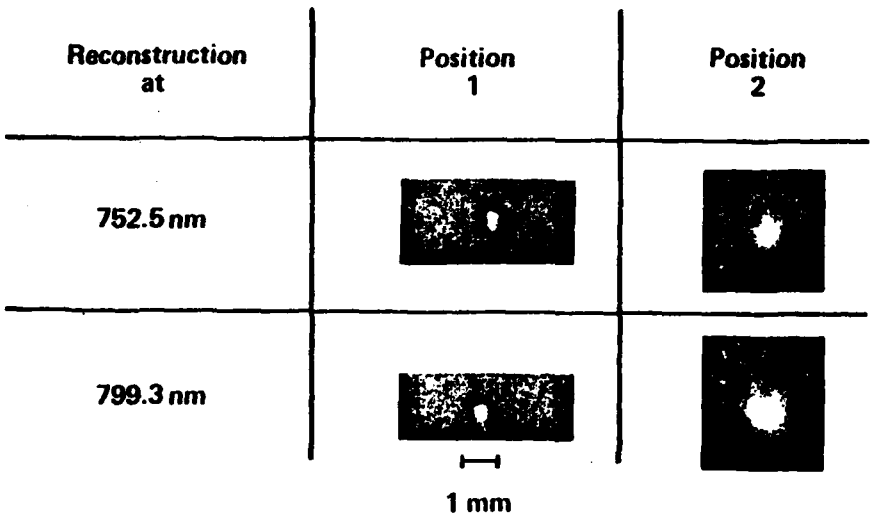

Figure 21. Two-photon holographic lens formed at 752.5 nm and reconstructed at two different wavelengths. Position 1 is near the focal point of the lens and Position 2 is beyond that point.

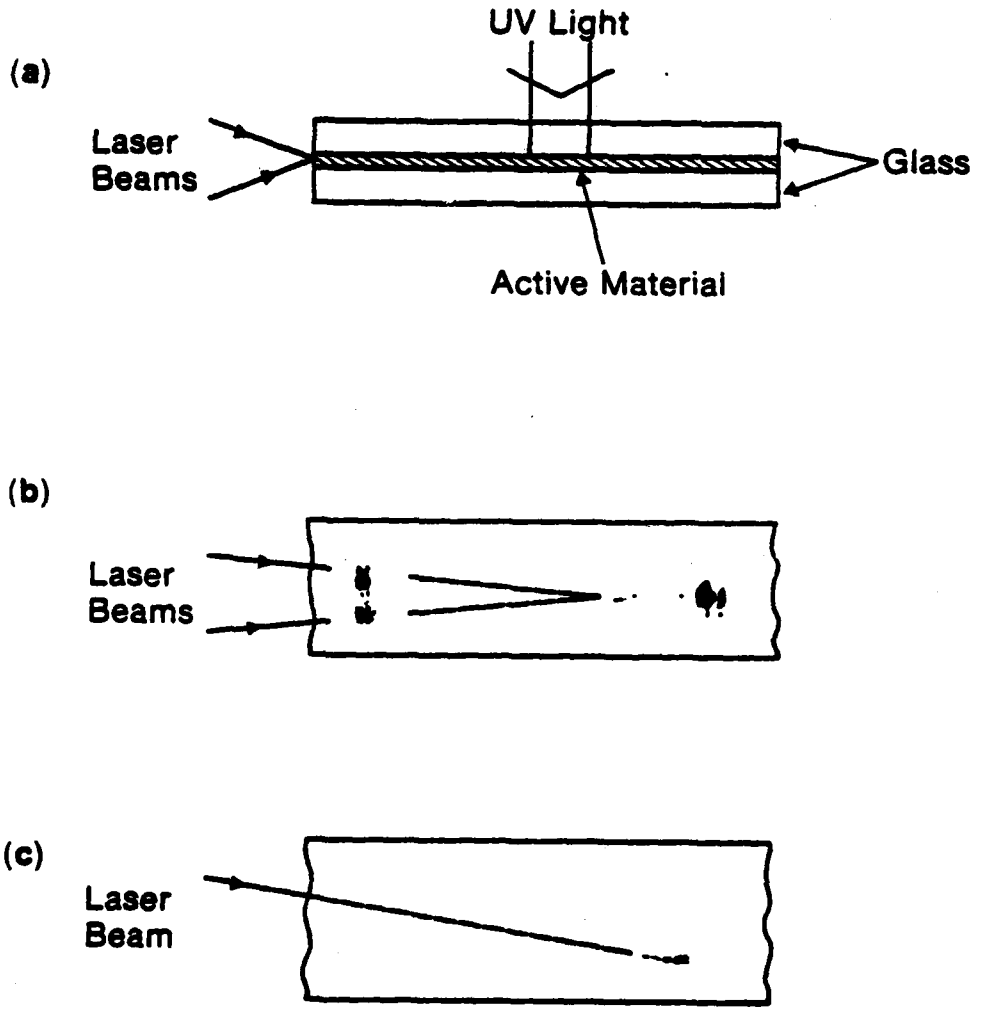

Figure 22. Formation of a thin film waveguide directional coupler using the 752.5 nm Kr^+ laser line. (a) A schematic diagram of the waveguide structure. (b) Recording of the directional coupler. (c) Reconstruction.